Bulletin of the New Zealand Society for Earthquake Engineering, Vol. 58, No. 1, March 2025

RECOMMENDATIONS FOR THE REVISION OF THE APPROACH FOR SEISMIC DESIGN OF PARTS AND COMPONENTS IN NEW ZEALAND DESIGN STANDARDS

Kieran Haymes[1], Timothy J. Sullivan[2] and John Hare[3]

(Submitted *August 2023*; Reviewed *November 2023*; Accepted *January 2024*)

ABSTRACT

This work makes recommendations for revision of the design provisions for the seismic demands on non-structural elements, parts and components in the New Zealand seismic loading standard. The proposed approach seeks to incorporate new and international knowledge of the factors affecting seismic demands on non-structural elements, but also maintaining simplicity to facilitate adoption. The most significant changes include new expressions for the influence of floor height and building nonlinear response on floor acceleration demands; the amplification of demands on flexible parts due to dynamic amplification associated with the response of structural modes; and potential reductions in part strength requirements by permitting nonlinear part response. The proposed revisions are supported by data from instrumented buildings, numerical modelling and experimental testing. Comparisons between the recommended and existing NZS 1170.5 approaches are presented that show that the proposed approach will lead to reduced design actions in many cases and increased loads in others. Greater demands are prescribed for flexible parts with limited ductile capacity and some parts at the serviceability limit state design level. Conversely, design forces reduce for rigid parts; parts and components on lower levels of buildings; ductile flexible parts; parts in ductile buildings at the ultimate limit state design; and parts with long periods. Finally, the proposed approach is compared with the most recent updates to the code design approaches in Europe and the United States to provide an international context of the state of the art.

https://doi.org/10.5459/bnzsee.1661

INTRODUCTION

Lessons from recent earthquakes, as well as new hazard information for New Zealand, have prompted reconsideration of code design requirements. Consequently, this paper recommends revisions of the design provisions in Section 8 Requirements for Parts and Components of the New Zealand seismic loading standard NZS 1170.5:2004 A1 [1].

Significant repair and disruption costs due to damage to parts and components (which include non-structural elements) were incurred following the strong ground motions in New Zealand in the last fifteen years, leading to losses even in moderate earthquakes where the structural elements have been largely undamaged [2–4]. These experiences emphasise the importance of the seismic performance of parts and components, which compose eighty to ninety percent of construction cost of new buildings [4]. Poor part performance heavily impacts the resilience of New Zealand's built environment, highlighting the need to address parts as resilience comes increasingly into the focus of the earthquake engineering profession beyond the current minimum standards for life preservation [5]. Though non-compliant and unrestrained parts can be attributed to many losses, engineers may be empowered to improve the seismic performance of parts and components by reliably estimating actions imposed by earthquakes. The present study is limited in scope to the horizontal loading on acceleration-sensitive components. Drift may be controlled during the design of the primary structure [6] and more research into vertical demands is recommended.

Literature on the seismic loading on parts and components has grown exponentially [6–15]. Some studies have proposed direct approaches that use simplified expressions which describe key parameters that affect seismic demands on parts and components [16; 17], whereas others derive the peak response of parts and components using floor response spectra constructed using superposed modes of the supporting structure [7; 18–22]. These efforts have lead to recently revised codes in the United States within ASCE 7-22 [23] and the imminent update to Eurocode 8 [24], with the former opting to maintain simplified expressions following the recommendations of the ATC-120 project [16] and the latter broadly adopting the modal superposition approach by Vukobratovic and Fajfar [20].

The development of technical standard TS1170.5 has provided an opportunity to address perceived shortcomings of the current approach for parts and components that have been identified in literature [21; 22; 25–27]. Functional objectives of possible revisions were identified by the authors in a workshop in 2022 where New Zealand engineering practitioners and academics expressed their views on the seismic demands on building parts and components [27]. This included perceptions from practitioners that the existing provisions were overly conservative but with academics pointing out instances where the provisions would be non-conservative. As such, the desire for new method with a rigorous scientific basis, simplicity and ease of use, reliability, and addressing perceptions of overly-conservative provisions were the drivers for the present work.

[1] *Corresponding Author, Postdoctoral Research Fellow, University of Canterbury, Christchurch, kieran.haymes@canterbury.ac.nz (Member)*
[2] *Professor, University of Canterbury, Christchurch, timothy.sullivan@canterbury.ac.nz (Member)*
[3] *CEO, Holmes Group, Christchurch, JohnH@holmesgroup.com (Member)*

In this paper, the recommended approach will be presented. The parameters that influence demands on parts and components within the proposed framework will be examined and discussed. Finally, the existing NZS 1170.5 approach will be compared with the recommended approach as well as those recently included in ASCE 7-22 and Eurocode 8. Example applications of the recommended approach are provided in the Appendix. Further detail on recommended and existing approaches, comparisons, and workshop outcomes is also available [27].

DATA USED FOR VERIFICATION

To validate the various provisions, comparisons were made with data from instrumented buildings and numerical modelling. These data sources are described in the subsections that follow.

Instrumented Buildings

The factors affecting seismic demands on parts and components within elastically responding structures is examined by considering bidirectional floor motions from recent earthquakes recorded by triaxial accelerometers under the GeoNet Structural Array instrumented building programme [28] as well as international literature. The structures examined in this work are the two seismically-separated Avalon GNS buildings (Units One and Two), the University of Canterbury Physics (UC Physics) building, the Ministry of Business, Innovation and Employment (MBIE) Stout St building, Wellington Hospital, the Nelson Marlborough Institute of Technology (NMIT) building, the Victoria University Te Puni Village building, and the Majestic Centre. Properties of these buildings are summarised in Table 1.

Motions of the UC Physics building due to the 2010/2011 Canterbury earthquake sequence (M4.7 to M6.3) were recorded, where minor cracking of the concrete structure was observed [29]. Motions were recorded in the 2013 Seddon (M6.5) and Grassmere (M6.6) earthquakes by the GNS, Wellington Hospital, NMIT, Victoria University, and Majestic Centre buildings. The 2016 M7.8 Kaikōura earthquake motions were recorded at the GNS, Wellington Hospital, NMIT, and MBIE buildings. All buildings are assumed to have responded without material inelasticity [2]. The observations from the instrumentation data are thus used in this study to represent realistic seismic loading on parts and components for elastic structural response.

Numerical Modelling

Considerations for nonlinear structural response are supplemented in this study using results from time history analyses conducted by Welch and Sullivan [21]. The response of steel moment resisting frame (therein referred to as stiff steel MRFs [21]) and reinforced concrete wall lateral load resisting systems were examined using RUAUMOKO3D [30] with two-dimensional centreline models of four-, eight-, and twelve-storey structures. The forty-four recorded ground motions comprising the FEMA P695 far-field set [31] were used to impose earthquake actions, scaled to six intensity levels using factors producing median peak ground accelerations from 0.15 g to 0.9 g. The steel MRF buildings were also run at 1.2 g.

In this study, results from these numerical models will be used to illustrate demands on parts and components where the structure exhibits both elastic and inelastic behaviour, which are characterised by effective system displacement ductility values, henceforth referred to as structural ductility values, μ. Structural ductility values were estimated by Welch and Sullivan [21] for each record in each building. Structural ductility values for the steel MRF buildings were estimated based upon the elastic strain energy, or "work-done", developed in the plastic hinge zones of the steel members. Structural ductility values were estimated for the RC wall buildings using the ratio of the maximum recorded displacement to the corresponding yield displacement, at the effective (equivalent SDOF) building height. Motions that resulted in structural ductility values within 15% of 1.0, 2.0, and 4.0 will be considered throughout the present work, and the quantity of motions for each case is given in Table 2. Further details on the structural models are given by Welch [32].

OVERVIEW OF THE RECOMMENDED APPROACH

To define the design actions on parts and components, the approach shown in Figure 1 is recommended. Design actions on parts and components are produced in discrete stages that consider the intensity of the demands at the ground, how the distribution of the demands at the floor levels are influenced by the response of the structure, and how parts and components respond to the floor motions. Firstly, the intensity of shaking is considered using the peak ground acceleration. Secondly, the way the peak floor demands varies throughout the height of the building is considered, initially as amplification of the peak ground acceleration when elastic structural response is consid-

Table 1: Overview of GeoNet [28] instrumented buildings used as case studies.

Building	Location	No. of storeys	Lateral load resisting system	Year built	Year instr.ed	Instruments available
University of Canterbury Physics	Christchurch	8	Coupled reinforced concrete shear walls	1961	2007	10
Avalon GNS Unit 1 & Unit 2	Lower Hutt	3	Reinforced concrete moment frame	1973	2007	4, 5
MBIE Stout St	Wellington	9	Concrete-encased steel moment frame	1940	2014	16
Wellington Hospital	Wellington	6	Base-isolated reinforced concrete moment frame	2008	2009	16
Nelson Marlborough Institute of Technology	Nelson	3	Timber shear walls with energy dissipating devices	2011	2011	9
Victoria University Te Puni Village	Wellington	10	Rocking steel moment frame	2009	2009	12
Majestic Centre	Wellington	28	Reinforced concrete shear walls	1990	2011	15

Table 2: Quantity of earthquake motions examined that resulted in structural inelasticity characterised by the three considered structural ductility values.

Building		Structural ductility value μ		
		$1.0 \pm 15\%$	$2.0 \pm 15\%$	$4.0 \pm 15\%$
RC Wall	4-storey	34	42	29
	8-storey	47	36	5
	12-storey	45	37	3
Steel MRF	4-storey	45	59	8
	8-storey	44	53	4
	12-storey	45	48	3

ered, followed by apparent reductions of floor motions when the effects of structural nonlinearity are considered. Subsequently, the response of the part or component is similarly considered, first as possible amplification of the peak floor acceleration, then as effective reductions of required part strengths by permitting nonlinearity in the part to develop. A final part or component reserve-capacity factor accounts for limit state design objectives. This approach seeks to maintain the existing NZS 1170.5 framework and minimises alterations where possible to facilitate its adoption by New Zealand engineering practitioners.

The recommended horizontal design earthquake action on a part, F_{ph}, is computed using Equation 1:

$$F_{ph} = \frac{C_p(T_p)}{\Omega_p} R_p W_p \leq \frac{[7.5PGA]}{\Omega_p} R_p W_p \tag{1}$$

where R_p is the part risk factor, as currently specified in NZS 1170.5; W_p is the weight of the part; and PGA is the peak ground acceleration; and Ω_p is the part reserve-capacity factor. The part reserve-capacity factor considers the ratio of the likely strength to the design strength and is recommended to be taken as 1.5 for the ultimate limit state (ULS), 1.25 for serviceability limit state 2 (SLS2) and 1.0 for the serviceability limit state 1 (SLS1), unless demonstrated to be greater. Ω_p should not be taken to be greater than 1.0 for brittle parts. Equation 1 also includes a design response coefficient for parts and components, $C_p(T_p)$, determined using Equation 2:

$$C_p(T_p) = PGA \left[\frac{C_{Hi}}{C_{str}}\right] \left[\frac{C_i(T_p)}{C_{ph}}\right] \tag{2}$$

where C_{Hi} is the floor-height coefficient, describing the amplification of demands felt by the floors relative to the ground; C_{str} is the structural-nonlinearity-reduction factor, describing the apparent reduction of demands due to nonlinear structural response; $C_i(T_p)$ is the part or component spectral-shape coefficient, describing the amplification of demands on the part relative to the floor as a function of the period of the part, T_p; and C_{ph} is the part-response or component-response factor, describing the reductions in strength requirements when nonlinear response of the part or component can be accommodated. An optional alternative approach for parts with long periods is also recommended later in this work. The following subsections will outline how the parameters in NZS 1170.5 may be modified to better represent behaviours observed in the literature.

Figure 2 demonstrates the application of the recommended approach for rigid, flexible, and long-period parts exhibiting elastic (μ_p = 1.0) and limited ductile (μ_p = 1.5) responses mounted at roof level of the UC Physics Building, comparing the predicted demands with the recorded roof and ground acceleration response spectra (normalised by PGA) recorded during the 2011 Lyttelton M6.2 earthquake. Discussion on the construction of the predictions and their performance demonstrated in this figure is provided throughout this paper in relevant sections.

FLOOR-HEIGHT COEFFICIENT

Quantification of Ground Motion Intensity

The effects of ground motion intensity are quantified in Equation 2 using the peak ground acceleration, PGA, at the consid-

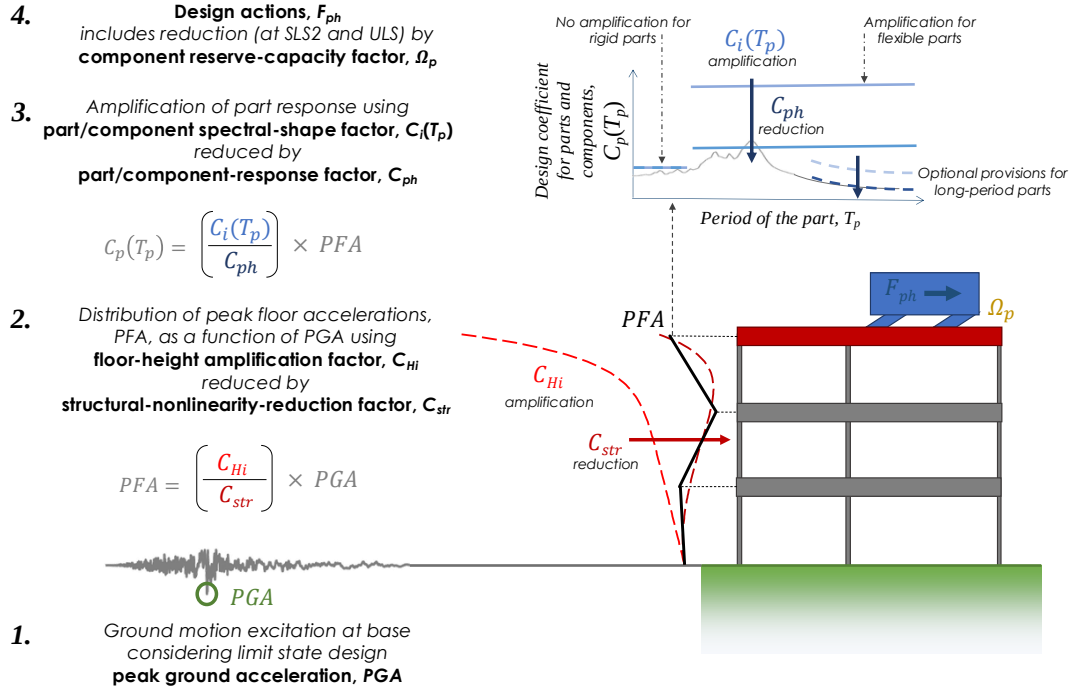

Figure 1: A schematic of the recommended framework for the consideration of demands on parts and components.

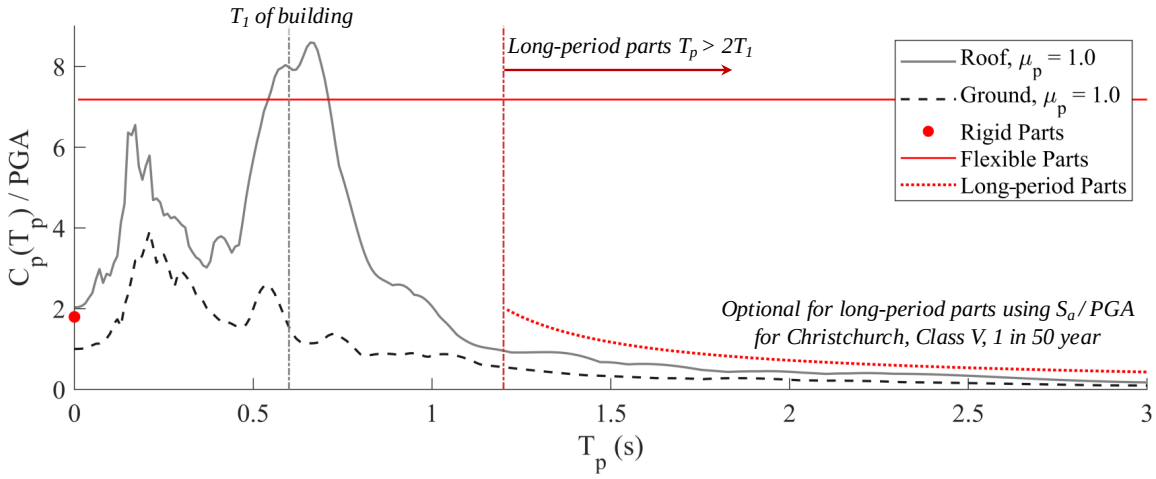

(a) Part ductility μ_p = 1.5.

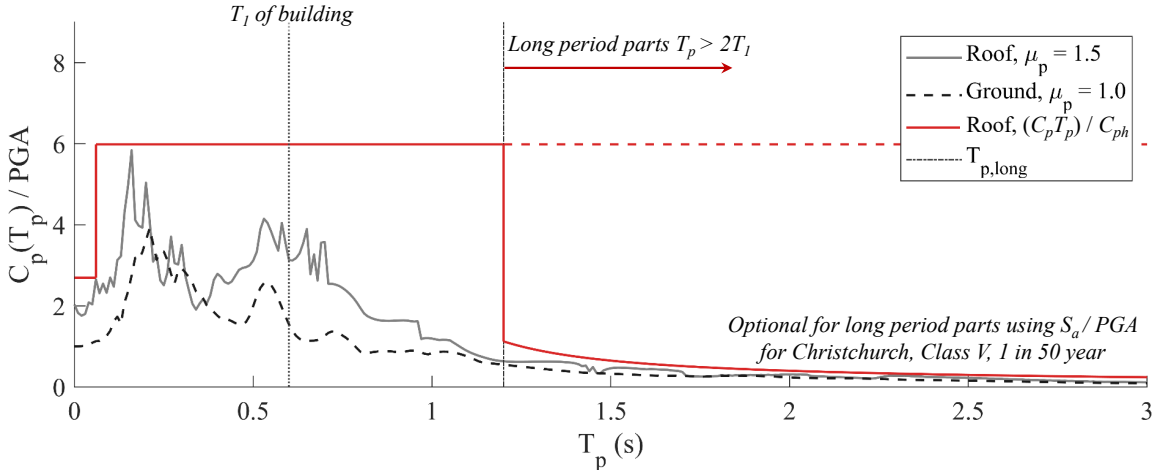

(b) Part ductility μ_p = 1.5.

Figure 2: Application of provisions for rigid, flexible, and long-period parts with the roof and ground acceleration response spectra (normalised by PGA) recorded in the UC Physics Building during the 2011 Lyttelton M6.2 earthquake.

ered limit state design intensity, as currently done in NZS 1170.5. This is similar to ASCE 7-22, where an effective peak ground acceleration is approximated using the short period spectral acceleration (therein referred to as S_{DS}, here as $S_{a,s}$) factored by 0.4, thought to better describe the structural response by eliminating the effects of high frequency ground responses [33]. Modal superposition methods for floor acceleration response spectra [7; 18–22] correlate peak floor accelerations with a combination of the ground spectral accelerations corresponding to the modal periods of the structure. Peak floor accelerations may not, therefore, be well represented by *PGA* or $S_{a,s}$ for tall and/or flexible buildings as structural response is often dominated by the response of the first structural mode. However, use of the *PGA* is simple and data from instrumented buildings has supported a new expression for the floor-height coefficient reported by the Applied Technology Council [16]. Further, maintaining consistency with the existing NZS 1170.5 provisions wherever possible is likely to help adoption of the recommended revisions.

Amplification of Demands with Floor Height

The dynamic response of the lateral load resisting system of a building, when elastic, has been widely observed to result in amplification of the motion of the floors relative to the ground, which tends to increase with floor height [7; 16–22; 34–36]. Miranda and Taghavi [34] observed that this amplification often decreases with greater fundamental structural periods. These behaviours are demonstrated in Figure 3, which shows the floor height distribution of recorded peak floor accelerations, normalised by corresponding peak ground accelerations, from four of the New Zealand instrumented buildings in two orthogonal directions. Although it is acknowledged that this is a limited data set, the distributions in Figure 3 appear similar to previous observations from larger data sets [16; 34].

To define how the peak ground acceleration is amplified to the floor levels of the structure as peak floor accelerations for elastic structural response, a new expression for the floor-height coefficient, C_{Hi}, is recommended for use in Equation 2. The recommended expression has been adopted directly from ASCE 7-22, which was derived from the recorded variation in the peak floor acceleration, normalised by peak ground acceleration, from over one hundred instrumented buildings in California and the mean (average) variation computed using simplified continuous models of a flexural beam laterally coupled with a shear beam [16]. C_{Hi} is hence defined using Equation 3:

$$C_{Hi} = 1 + \frac{1}{T_1}\left(\frac{h_i}{h_n}\right) + \left[1 - \left(\frac{0.4}{T_1}\right)^2\right]\left(\frac{h_i}{h_n}\right)^{10} \qquad (3)$$

where h_i is the height of attachment of the part from the base of the structure, h_n is the height from the base of the structure to the uppermost seismic weight or mass in the structure, and T_1 is the

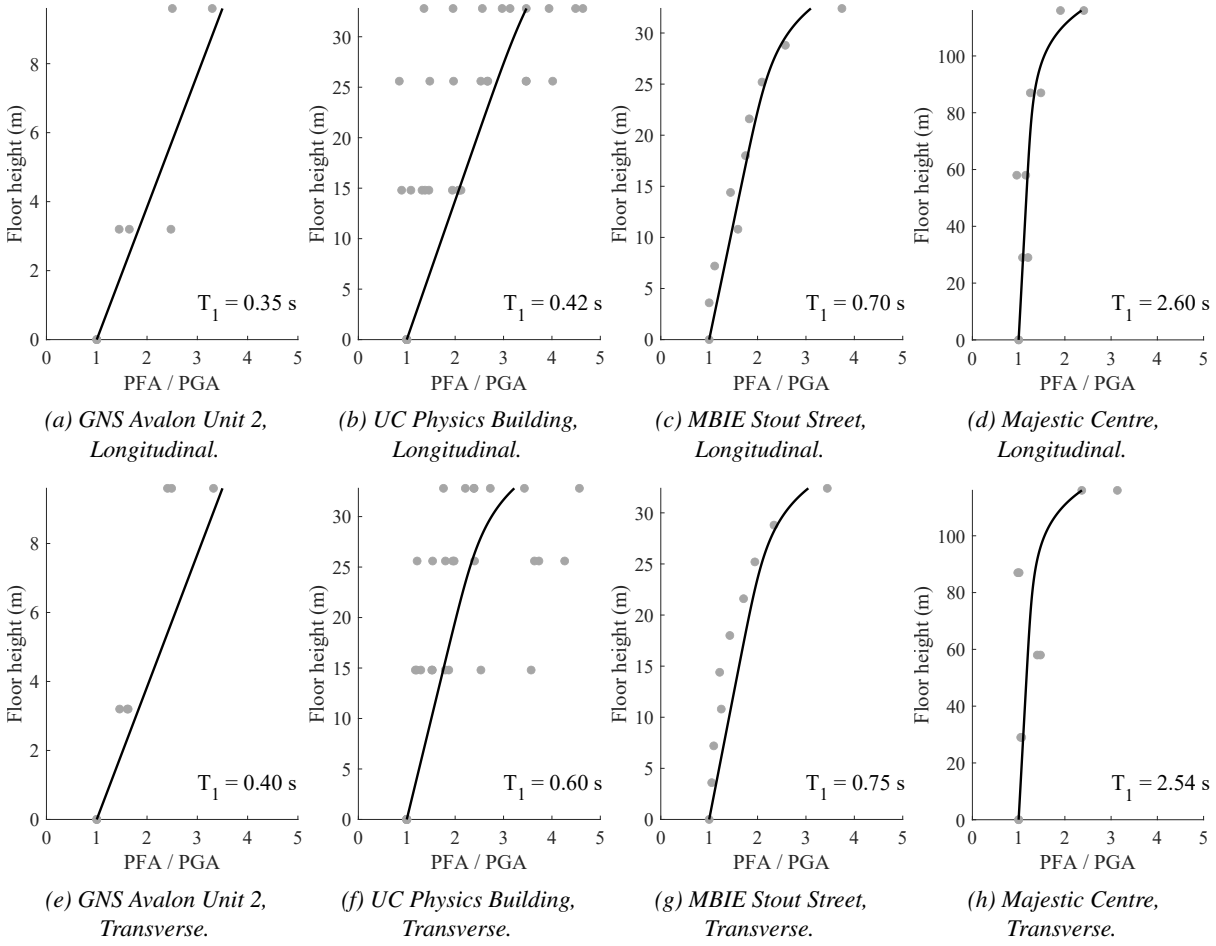

(a) GNS Avalon Unit 2, Longitudinal. *(b) UC Physics Building, Longitudinal.* *(c) MBIE Stout Street, Longitudinal.* *(d) Majestic Centre, Longitudinal.*

(e) GNS Avalon Unit 2, Transverse. *(f) UC Physics Building, Transverse.* *(g) MBIE Stout Street, Transverse.* *(h) Majestic Centre, Transverse.*

Figure 3: Distribution of peak floor accelerations, normalised by corresponding peak ground accelerations, recorded in instrumented case study buildings. The recommended floor-height coefficient, C_{Hi}, is shown.

largest translational period of vibration of the primary structure in the direction being considered. Equation 3 may be applied if T_1 can be demonstrated to be longer than 0.4 seconds. If T_1 is equal to or less than 0.4 seconds, or unknown, the floor-height coefficient should instead be calculated using the simple form in Equation 4:

$$C_{Hi} = 1 + 2.5\left(\frac{h_i}{h_n}\right) \tag{4}$$

Equation 4 states that the amplification of the peak floor acceleration, relative to the peak ground acceleration, increases linearly from 1 to 3.5 for structures with fundamental structural modal periods below 0.4 seconds, which is equivalent to the limits specified in the ATC-120 report [16], adopted in ASCE 7-22. This is the most conservative distribution of demands and is therefore able to be used without requiring any knowledge of the modal characteristics of the structure. If the fundamental period can be demonstrated to be greater than 0.4 seconds, Equation 3 can be used and will result in reduced demands with longer periods, forming a hooked shape, as shown in Figure 4.

Using these provisions, design may be conducted on a storey-by-storey basis or by simply considering the loads at the roof level. In seeking to accurately describe the distribution of loads with floor height, designers can be incentivised to locate key pieces of equipment where they are expected to attract lower seismic demands.

In lieu of more robust estimates, simplified empirical expressions for approximating the fundamental period of structures may be

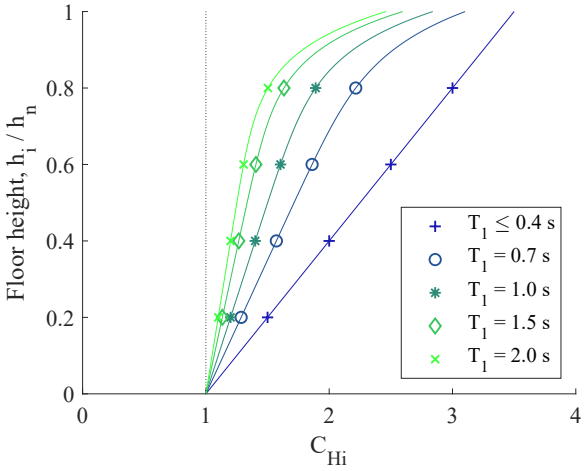

Figure 4: The distribution of demands with floor height, C_{Hi}, for values of the fundamental structural period, T_1.

employed, including the approach provided in Section C4.1 of the commentary to NZS 1170.5 [37] which uses the total height the building and a coefficient configured for different lateral load resisting systems. These expressions tend to underestimate the building period, and should therefore provide conservative values for the floor-height coefficient. The fundamental period of the structure may also be influenced by foundation flexibility, soil stiffness and non-structural components, which may not always be modelled explicitly when estimating structural modal properties.

In Figure 3, the recommended expression for the floor-height coefficient is compared with the peak accelerations of the floors relative to the ground, *PFA*/*PGA*, recorded in the instrumented buildings. The predicted distribution in the GNS Avalon Unit Two building, from 1 to 3.5, is slightly more conservative than recorded observations. For taller buildings, with longer fundamental periods, the recommended C_{Hi} values appear to adopt similar values to the observed distribution of demands. The recommended C_{Hi} values will often be less conservative than those provided in NZS 1170.5, which commonly prescribes a value of 3.0 at floors above 20% of the total building height. The wide dispersion of demands in the UC Physics Building data, in Figures 3b and 3f, evidences the large level of uncertainty in the estimation of demands with height, which has been observed elsewhere [16; 17; 34–36].

The recommended expression for the peak floor acceleration distribution over the lower half of the structure provides values that are significantly lower than the provisions in NZS 1170.5 for buildings with a total height of greater than 12 metres. This may be due to NZS 1170.5 assuming that higher structural modal response will result in very large amplifications over lower levels. This assumption appears to be based upon an envelope of peak floor acceleration distributions computed from the results of time history analysis of three reinforced concrete structures by Shelton [17]. There, peak floor accelerations are normalised by the NZS 1170.5 elastic hazard, $C(0)$, instead of the peak ground acceleration of each record. Other studies considered herein [16; 34–36] which have examined results from numerical analysis and data from instrumented buildings have not observed significant amplifications over lower building levels.

While the recommended approach for the definition of the peak floor motions relative to peak ground motion in Equations 3 and 4 is considered to provide a suitable estimate for code design purposes, the *PFA*/*PGA* ratio can be affected by factors that are not explicitly considered. It is known that higher mode demands will contribute to the *PFA* demands and that the relative importance of higher modes can change with ductility demand, intensity, spectral shape and building characteristics [16; 20–22; 38]. Buildings with significant torsional behaviour will also tend to develop larger *PFA* demands at the building perimeter, on the order of approximately 1.2 [16]. Diaphragm flexibility can also amplify demands between lateral load resisting elements [16; 39]. This behaviour may result in similar floor demands as those expected for flexible parts, as discussed later in this paper.

Single-Storey Buildings

The application of Equation 4 for single-storey structures results in a floor-height coefficient at the roof of 3.5. A structure that may reasonably be modelled as a single-degree-of-freedom system with a short period, as expected for single-storey building, may be expected to experience a peak acceleration corresponding to the constant acceleration region of the design ground response spectrum, which will be referred to as the short period spectral acceleration, $S_{a,s}$, in the proposed technical standard. Consequently, the floor-height coefficient may be described as the ratio of $S_{a,s}$, to the peak ground acceleration, *PGA*, determined considering the local seismic hazard. This may be on the order of 2.5 or less. This approach is likely conservative for the unusual case that a single-storey buildings possesses a period greater than T_C, which defines the short period spectral acceleration plateau.

STRUCTURAL-NONLINEARITY-REDUCTION FACTOR

When a SDOF structure yields, the effective lateral force, and hence acceleration, is limited [6]. Thus, it can be expected that when structures respond nonlinearly, floor accelerations will not continue to increase in proportion to the peak ground acceleration. Indeed, numerical studies of MDOF structures have observed that the proportion of floor acceleration demands associated with the fundamental structural response reduce approximately proportionally to structural ductility [21; 22; 40]. However, floor acceleration demands due to higher mode response are not likely to be as significantly affected by ductility, but overall, even for multi-storey buildings, the ratio of *PFA* to *PGA* has been seen to reduce with increasing levels of nonlinear response of the structure [16; 21; 22; 40; 41].

In light of these considerations, a structural-nonlinearity-reduction factor, C_{str}, is introduced into Equation 2, to limit the elastic amplification of *PFA*/*PGA* given by C_{Hi} due to structural nonlinearity, developed through material inelasticity or geometric nonlinearity. C_{str} is computed using Equation 5:

$$C_{str} = [C_{str,max}]^{e_{str}} \tag{5}$$

where $C_{str,max}$ is the maximum structural-nonlinearity-reduction factor, determined using Equation 6; and e_{str} is the floor height distribution exponent for structural-nonlinearity-reduction, determined using Equation 7:

$$C_{str,max} = \sqrt{\mu} \geq 1.3 \tag{6}$$

$$e_{str} = \left(\frac{h_i}{h_n}\right)^{1.5} \tag{7}$$

where μ is the structural-ductility factor for the structure as a whole at the design limit state, taken as 1.0 at SLS; h_i is the height of attachment of the part from the base of the structure, h_n is the height from the base of the structure to the uppermost seismic weight or mass in the structure. Figure 5 shows the distribution of the structural-nonlinearity-reduction factor with floor height.

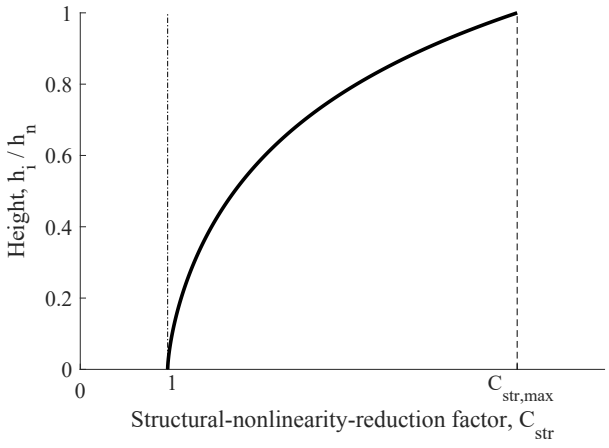

Figure 5: Structural-nonlinearity-reduction factor distribution with part attachment height.

As the assumed design ductility may often be larger than the actual ductility demand, and because contributions from higher modes are not as affected by ductility, the maximum reduction due to structural nonlinearity, $C_{str,max}$, described in Equation 6 is taken as the square-root of the design ductility. The recommended lower bound value of 1.3 acknowledges that some nonlinear response is expected, even for lower levels of excitation. This may include foundation response, cracking or slip

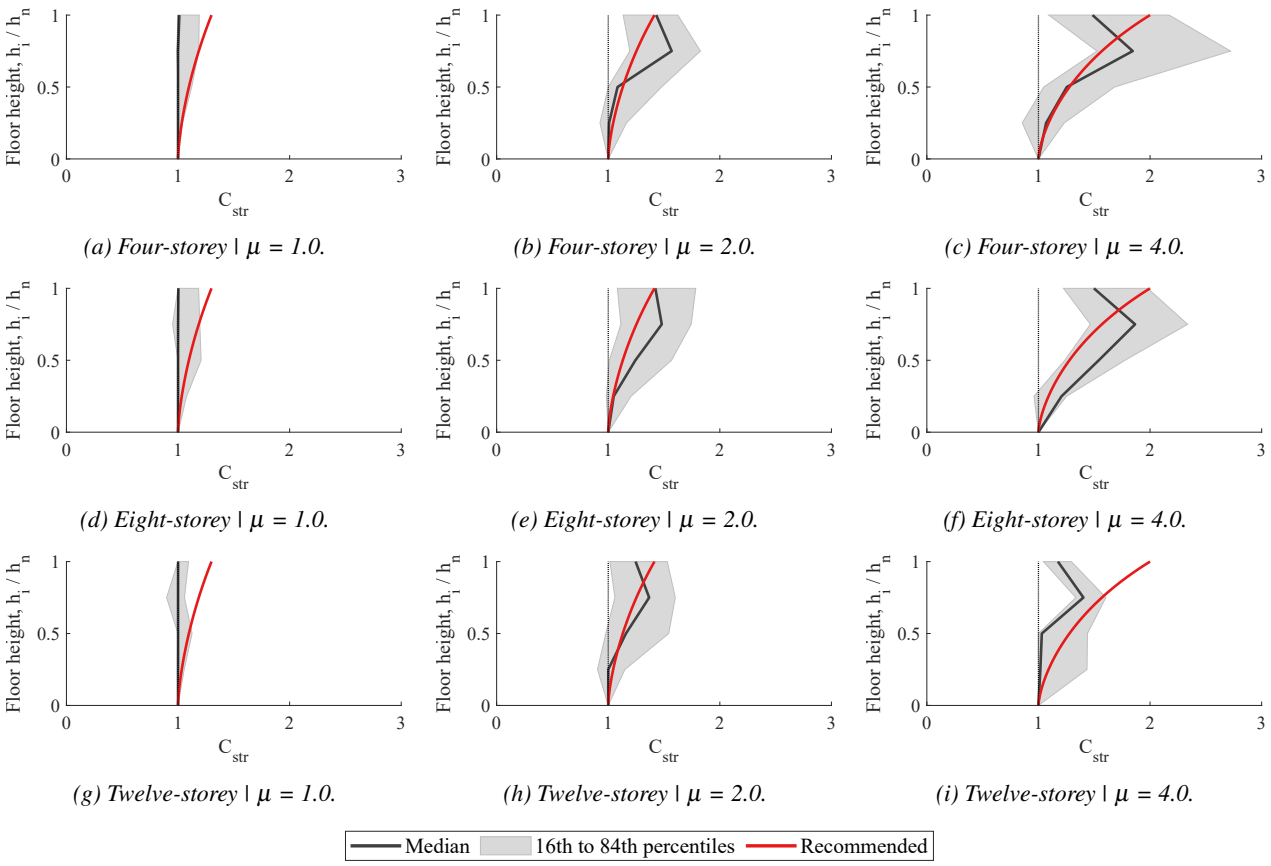

Figure 6: Distribution with height of the structural-nonlinearity-reduction factor in the RC wall structures.

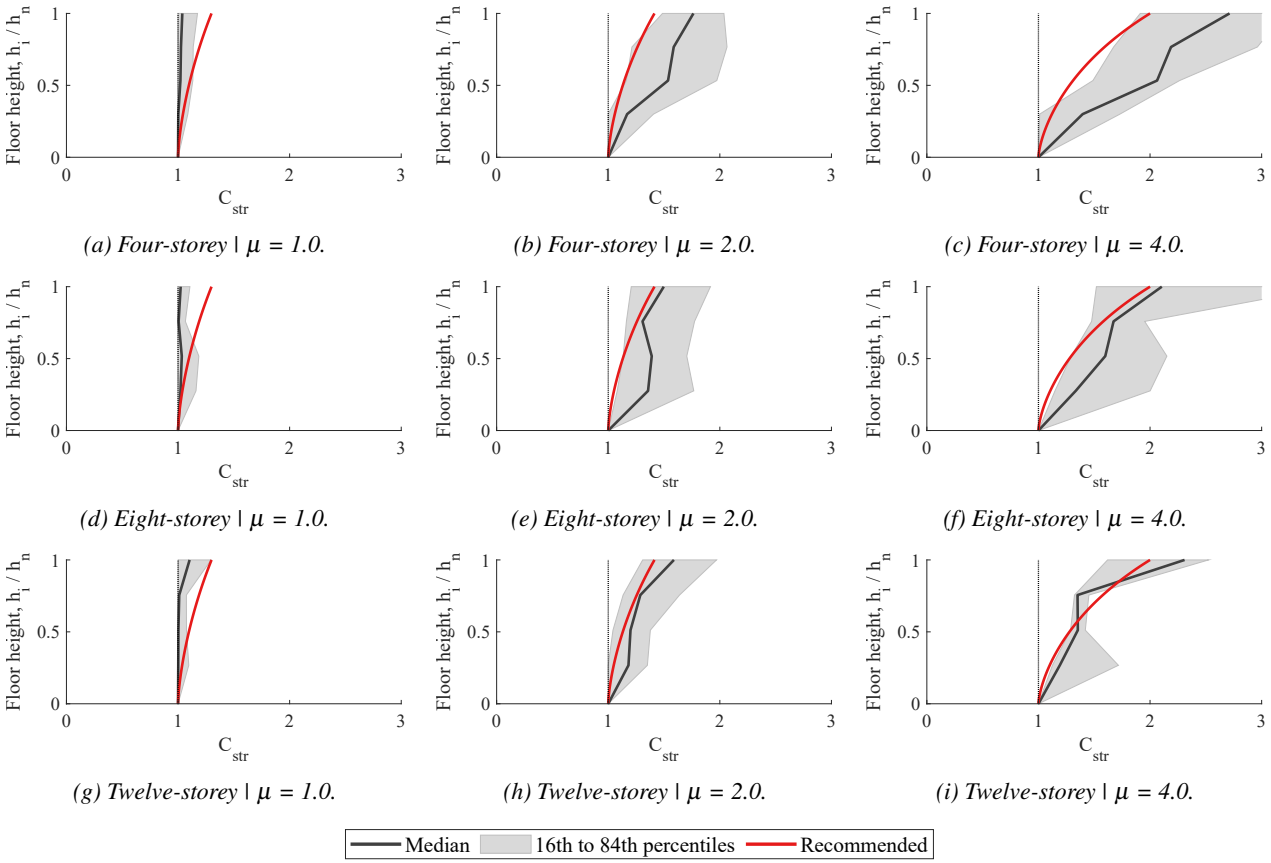

Figure 7: Distribution with height of the structural-nonlinearity-reduction factor in the steel MRF structures.

of structural elements and connections in the elastic range and interaction of the structure with non-structural elements. The recommended maximum reduction is equivalent to the ASCE 7-22 provisions for structural nonlinearity.

The approach recommended in Equation 5 reduces demands as a function of height, whereas ASCE 7-22 does not. By applying the maximum reduction to all levels, the ASCE 7-22 approach may result in non-conservative estimates of the peak floor accelerations over the lower levels of the structure, which tend to be controlled by the peak ground acceleration [27; 42].

The performance of the structural-nonlinearity-reduction factor can be gauged via Figures 6 and 7, which show the distribution of C_{str} with height in the RC wall and steel MRF structures [21], respectively, for the motions that resulted in structural ductility values of 1.0, 2.0, and 4.0 summarised in Table 2. The reduction factors describe the ratio of peak floor acceleration *PFA* distribution with floor height from time history analysis results that produced structural ductility values within 15% of the specified value (i.e.: μ of 1.0, 2.0, or 4.0), with the *PFA* from running the same ground motion scaled to the lowest considered peak ground acceleration *PGA* of 0.15 g. This provides a comparison of the nonlinear and elastic structural responses with the same ground motion frequency content. In Figures 6 and 7, the median, sixteenth, and eighty-fourth percentiles from the time-history results are shown.

Figures 6a, 6d, 6g, 7a, 7d and 7g, show the distribution of reductions from motions where the structures exhibited responses near the approximated yield strength (i.e., μ of 1.0). The reductions from the time history analyses are close to 1.0 at most levels of the structures, whereas the recommended reduction increases with height to the $C_{str,max}$ lower bound of 1.3 at the roof. This discrepancy is expected, however, as the recommended approach considers sources of nonlinearity that are expected to limit the *PFA* values even at low intensity levels that have not been included in the numerical models.

The recommended provisions for the structural-nonlinearity-reduction factor produce values that are lower than the median reductions for motions resulting in structural ductility values of 2.0 and 4.0 in both structures, indicating that the proposed revisions will often result in conservative estimates of the *PFA*/*PGA* ratio. This excludes the roof level of the RC wall at μ of 4.0, where reductions are greater near three-quarters of the height of the structure than the roof. This behaviour is likely due to higher mode responses which are not effectively reduced by the development of nonlinearity at the base of the RC wall, which appear particularly significant in the twelve-storey building in Figure 6i. In the steel MRF structures, conversely, the distribution of plastic hinge zones in the beam ends throughout the structure may limit the development of higher mode responses more effectively, resulting in greater reductions than estimated by the recommended approach. Variation in the extent of the reductions is observed in all cases, highlighting the uncertainties inherent in ground motion frequency, development of structural modal responses and inelasticity, and the characterisation of structural ductility demands.

PART OR COMPONENT SPECTRAL-SHAPE COEFFICIENT

The peak acceleration of an elastic part or component, relative to the peak floor acceleration, *PFA*, will depend on the dynamic properties of the part itself. This behaviour, referred to as dynamic amplification, has been observed to result in significant magnification of demands on the part when the period of the part is near the periods of the modes of the building, which can greatly increase with decreasing damping of the part and the building [8; 16; 18; 20; 21; 26; 43].

The effects of period and damping values on dynamic amplification are demonstrated in Figure 8, where the median and sixteenth to eighty-fourth percentile distributions are shown for roof acceleration response spectra normalised by their corresponding peak floor accelerations, for motions recorded in the case study New Zealand instrumented buildings. The spectra were computed for damping ratios of the part or component of 2%, 5%, and 10%. Rigid parts with very short periods experience no dynamic amplification. Flexible parts often experience the greatest dynamic amplification when the period of the part is close to the fundamental period of the building (i.e.: $T_p = T_1$), and may experience significant amplification near higher modal periods, as shown by the local maxima in the floor response spectra near the first and second modal periods of 0.60 s and 0.20 s exhibited by the UC Physics Building in Figure 2a. Dynamic amplification can also been observed in Figure 8 to decrease as the ratio of the part and fundamental building period increases.

Simplified Distinction between Rigid and Flexible Parts

The period of the part and the periods of vibration of the supporting structure are key parameters when characterising dynamic amplification. However, there are many complicating factors when approximating the period of the part. This includes sub-assemblies, nonlinearity resulting in period elongation, connections, anchorage, and the presence of different vibrational properties in different loading directions [33; 44; 45]. It is also uncommon for practitioners to have reliable estimates of the period of parts owing to their variety.

Because of uncertainty in period estimates and the desire from industry for an approach that does not require the estimation of part or the structure's higher modes, it is assumed in this work that any flexible part may experience dynamic amplification. It is recognised that if a part happens to have a period that is significantly different from the natural periods of the supporting structure, and if the structural characteristics do not change during shaking then the demands would not be as large. However, calculation of Tp is difficult or impractical for most parts, whereas T1 for the primary structure can be calculated from empirical formulae and checked via analysis, with suitable allowance for cracking. Furthermore, as the primary, secondary and NSE systems go through varying degrees of demand and potentially nonlinear response, the potential increases for period shift resulting in some degree of amplification as resonance or near resonance results. As such, unless a part is completely rigid, it is likely that some flexible parts will be in resonance with one of the modes of vibration in the structure and thus should be designed for demands that are amplified appropriately

Consequently, the definition of whether a part is rigid or flexible is a key challenge for the implementation of the recommended approach. This binary classification appears in previous versions of ASCE 7, but was altered in ASCE 7-22 to match the ATC-120 amplification framework which is based upon the likelihood of a part being in resonance with the fundamental mode of the building. Although ATC-120 and ASCE 7-22 defined this using bounds of the ratio of the period of the part to the fundamental structural period of 0.5 to 1.5, the tabulated component resonance ductility factor, C_{AR}, appears to have considered short and stiff buildings with relatively short periods, resulting in the same rigid/flexible framework as previous versions, although it is not clear how values in the tables that specify C_{AR} were formulated. The period ratio definition may also be unsatisfactory, as significant dynamic amplification associated with higher structural modes with periods shorter than half the fundamental period

have been frequently observed [8; 16; 18; 20; 21; 26; 43].

By classifying parts as rigid or flexible, the period of the part is not explicitly required. Guidance on the classification of parts and components as likely rigid or flexible may be provided in tables, as implicitly provided in the C_{AR} values in ASCE 7-22 (see also Appendix A of [27]). The diversity of parts and components means a prescriptive approach to classification of parts as rigid or flexible with tables offers only limited insight into expected response, however. Classification of components using tables should be conducted with caution, as practitioners may inaccurately characterise components as rigid if they are unfamiliar with the relevant dynamics. This may be mitigated by imposing limitations to the parts that can assumed to be rigid through the basis of their dimensions or properties [44]. Although the range of periods that can be considered short may be dependent on the properties of the supporting structure, parts with periods less than 0.06 s have been considered unlikely to exhibit dynamic amplification in previous work [16; 23].

Maximum Dynamic Amplification

It is clear from the data presented in the current study and previous work [6; 7; 21; 22] that the selection of damping values of the structural system and of the part or component will significantly influence the expected maximum dynamic amplification. Despite efforts to assess part damping values through experimentation, where some have observed values between 0.5% and 30% [45–48], there remains limited characterisation of the damping of many parts and components owing to their variety. This is especially pertinent for the high ground motion intensities that are most relevant for design, where damping effects may be expected to be greater. Consequently, this work follows the approach by the ATC-120 project [16] to consider a 5% part damping value to derive amplification values.

Recommended Approach for Part or Component Spectral-Shape Coefficient

The part or component spectral-shape coefficient, $C_i(T_p)$, describes the maximum dynamic amplification of the acceleration response anticipated for a part of component, relative to the peak floor acceleration, and is given in Table 3.

Table 3: Recommended part or component spectral shape coefficient, $C_i(T_p)$.

Rigid parts	**Flexible parts**	
All levels	At or below ground level	Above ground level
1.0	$\frac{S_{a,s}}{PGA}$	4.0

The recommended value for the part or component spectral-shape coefficient, $C_i(T_p)$, for rigid parts of 1.0 specifies that no dynamic amplification is anticipated. This is half of the current NZS 1170.5 provisions, which currently specify a conservative value of 2.0 which may have reflected the code-writers' perceptions that very few components will be truly rigid, and, to avoid negative impacts associated with a designer underestimating the real period of a component, the demands at zero period are set to reflect those more likely at short periods.

The recommended value for the part or component spectral shape coefficient, $C_i(T_p)$, for flexible parts mounted above ground level of 4.0 is compared against the observed dynamic amplification from the instrumented building data in Figure 8. This value was derived from the formulation by Haymes et al. [22], based on observations from instrumented buildings, applied using structural and part damping values of 5%. This resulted in a part or component spectral shape coefficient of 3.75, which was rounded to 4.0. This can be observed in Figure 8 to provide a value close to the median peak amplification at $T_p = T_1$ for 5%-damped parts, but varies greatly from the observed amplifications for the other part damping values, emphasising the significant effect of part damping on dynamic amplification. A similar value was recommended in the approach by the ATC [16].

The recommended values differ from the NZS 1170.5 provisions for $C_i(T_p)$, which has a trilinear shape which varies from 2.0 to 0.5 as a function of the period of the part. The formulation of the NZS 1170.5 spectral-shape coefficient by Shelton [17] appears to envelope the floor response spectrum shape that was considered typical based upon observations from numerical and instrumented buildings that experienced structural ductility.

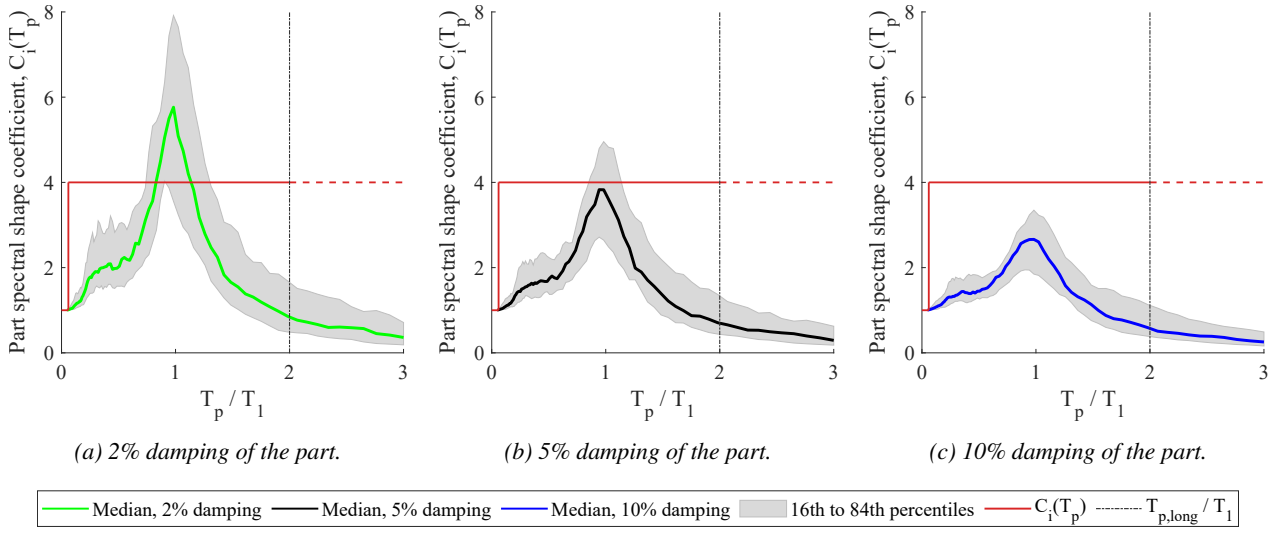

(a) 2% damping of the part. *(b) 5% damping of the part.* *(c) 10% damping of the part.*

Figure 8: The sixteenth, fiftieth, and eighty-fourth percentiles of the maximum dynamic amplification recorded in seven instrumented buildings in New Zealand [28], described by the roof spectral accelerations, $C_p(T_p)$, normalised by the corresponding peak floor accelerations, PFA, computed at three values for the damping of the part. The recommended part or component spectral-shape coefficient, $C_i(T_p)$, is shown, with the dashed line denoting that beyond the threshold long period, $T_{p,long}$, here equal to $2T_1$, the optional long-period provisions should be used if possible.

Significant structural nonlinearity is not expected at the serviceability limit state (SLS) intensity, however, at which the NZS 1170.5 approach for estimating the demands on parts is often applied. Instead, dynamic amplification is likely better represented by the data in Figure 8, computed from motions recorded in buildings that exhibited elastic behaviour.

Ground-Mounted Parts

Parts or components mounted at or below ground level will not be influenced by the response of the structure. Instead, modelled as a SDOF, the maximum elastic spectral acceleration, that may be developed for ground-mounted parts is equal to the constant short period spectral acceleration, $S_{a,s}$. Recall that, for elements at the ground level, the floor-height coefficient and the structural-nonlinearity-reduction factor, are set to one. Consequently, the maximum dynamic amplification described by $C_i(T_p)$ is recommended to be set as the ratio of the short period spectral acceleration and the peak ground acceleration, $S_{a,s}/PGA$, as given in Table 3. This is analogous to the reasoning used to derive the floor-height coefficient, C_{Hi}, for single-storey structures. Similarly, this approach is likely conservative for the case that a ground-mounted part possesses a period greater than T_C, which defines the short period spectral acceleration plateau.

PART-RESPONSE OR COMPONENT-RESPONSE FACTOR

Benefits of Permitting Ductile Part Response

Permitting nonlinear behaviour of parts and components allows for the design of the parts and their restraints to lower strengths than is needed to remain elastic under earthquake loading. Non-structural design approaches based on elastic floor acceleration response spectra can be conservative for parts that can respond nonlinearly. This can be observed by comparing the required part strength normalised by the peak ground acceleration, $C_p(T_p)/PGA$, for parts to remain elastic (μ_p = 1.0) with the strength requirements for parts that exhibit nominal ductility (μ_p = 1.5) computed from the recordings at the roof level of the UC Physics Building during the 2011 Lyttelton M6.2 earthquake shown in Figures 2a and 2b, respectively. All demands can be observed to decrease with increasing part ductility, particularly near the structural modal periods near 0.6 s and 0.2 s, except for rigid parts, as the peak floor acceleration remains unaffected.

The recommended part-response or component-response factor, C_{ph}, prescribes the effective reduction expected due to nonlinear part response, characterised by taking the ratio of the elastic and nonlinear strength requirements. As can be observed in the example in Figure 2, and widely recognised in literature [15; 16; 22], the effective reduction is closely related to the proximity of the period of the part to those of the structural modes. This is further demonstrated in Figure 9, which shows the median reduction factors observed in the records from the GNS Avalon, UC Physics, and MBIE Stout St instrumented buildings. Inelastic spectra were computed for part damping values of 2%, 5%, and 10% at part ductility values of 1.2, 1.5, 2.0 and 3.0, applying a con-

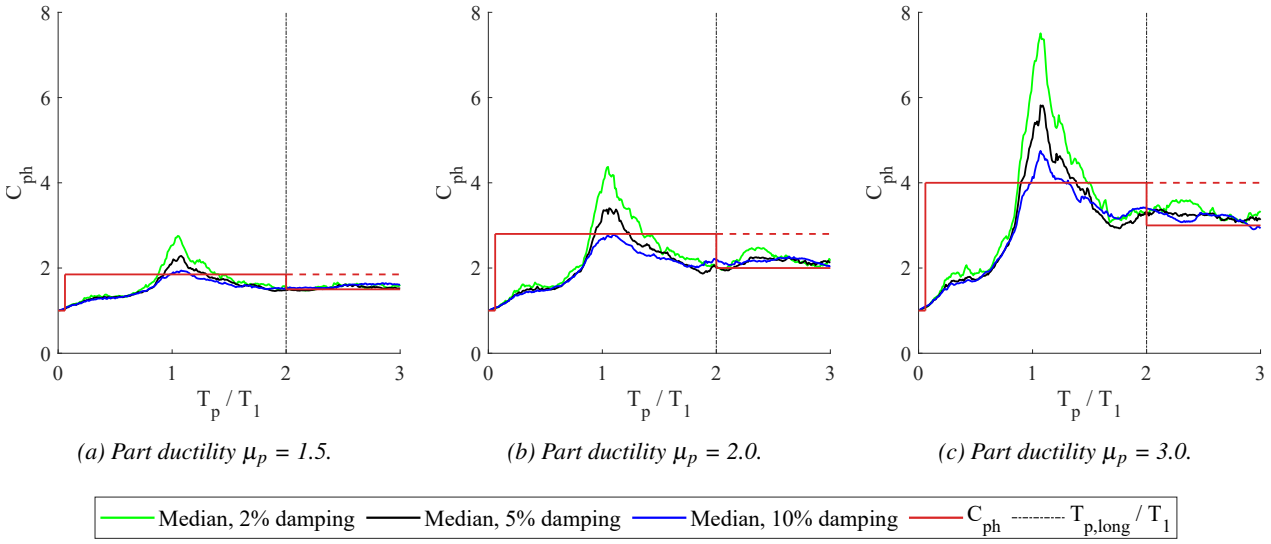

(a) Part ductility μ_p = 1.5. *(b) Part ductility μ_p = 2.0.* *(c) Part ductility μ_p = 3.0.*

Figure 9: Median force reduction factors using instrumented building records. Inelastic spectra were computed at part damping values of 2%, 5%, 10% for allowable part ductility values of 1.5, 2.0 and 3.0 using an elastic-perfectly plastic hysteresis. The recommended part-response or component-response factor, C_{ph}, is indicated, noting that beyond the threshold long period, $T_{p,long}$, the optional long-period provisions should be used if possible.

Table 4: Recommended part or component part response factor, C_{ph}.

Ductility of the part, μ_p	**Rigid parts** All levels	**Flexible parts** At or below ground level	**Flexible parts** Above ground level	**Long-period parts** All levels
1.0	1.0	1.0	1.0	1.0
1.25	1.0	1.25	1.4	1.25
1.5	1.0	1.5	1.85	1.5
2.0	1.0	2.0	2.8	2.0
2.5 or greater	1.0	2.5	4.0	2.5

stant damping ratio coefficient retaining the initial elastic value and using an elastic-perfectly plastic hysteresis. An integration time step of 0.001 seconds was adopted. Rigid parts are not expected to experience amplification or reductions, and the term $[C_i(T_p)/C_{ph}]$ is equal to one in all cases. As shown and discussed in the previous subsection, elastic flexible parts and components may experience significant dynamic amplification, particularly if they have low damping. Using instrumented building data, including the results presented in Figure 9, Haymes et al. [22] proposed that the design yield force could be approximated to have a reduction equal to the permitted ductility of the part raised to the power of 1.5, $\mu_p{}^{1.5}$, for the dynamic amplification associated with the response of the part to the fundamental structural mode, which was considered for the derivation of $C_i(T_p)$ for flexible parts. Haymes et al. [22] approximated the reduction to be equal to the permitted ductility of the part, μ for for parts mounted at the ground level, and for parts with periods significantly greater than the fundamental structural mode, referred to in this paper as long-period parts and discussed in a later section.

The observed behaviours in Figure 9, in previous work by the authors [22], and in other work [15; 16] lead to the values provided in Table 4, which follows the tabulated form in the current NZS 1170.5 approach, but with some significant changes. Firstly, it should be noted that the part-response or component-response factor was used as a coefficient in the general design expression in NZS 1170.5, and thus adopted values equal to or less than one. The recommended approach, conversely, proposes the use of the part-response or component-response factor as a reduction factor for the elastic amplification. This is described by the part or component spectral-shape coefficient within the expression for design the response coefficient for parts, $C_p(T_p)$, in Equation 2, and thus has values equal to or greater than one. The recommended part-response or component-response factor distinguishes between rigid and flexible parts, whereas the NZS 1170.5 approach applies the same coefficient for all parts, independent of the period of the part or structure. The values computed using these expressions are rounded to the nearest 0.05 to provide the recommended C_{ph} values in Table 4. These values are similar to those other work [15; 16].

Considerations for Estimating the Part Ductility Factor

Part ductility through nonlinearity, either through material inelasticity or geometric nonlinearity like rocking, bolt slip, or sliding, may be developed to act analogously to inelastic displacement for these small systems. Part ductility is therefore used as a proxy to refer to the ability of the part to reduce dynamic amplification through nonlinear response. The characterisation of part ductility values in various codes are not supported with significant research and have instead relied largely upon judgement. While existing codes [1; 23] suggest shake table testing for verification, this may not be practical for the vast multiplicity of parts and components. Table 5 provides generalised descriptions that may assist in the estimation of permissible ductility values.

Although it is acknowledged that characterisation of part ductility values is an area requiring further research, recommendations for part ductility values for design at the ultimate limit state (ULS) are shown for some key parts in Table 6. Although the part design ductility refers to the ratio of the displacement capacity to the displacement at yield, the displacement capacity for ULS may be higher than the inelastic deformation alone due to contributions from connection slip and the level of redundancy in the part or component system. Indeed, the values recommended in Table 6 reflect the expected ductility characteristics described in Table 5 based on experimental observations in the supporting literature where available. These values are provided to facilitate the computation of the part-response or component-response factor, C_{ph}, and may therefore differ from observed ductility values.

Table 5: Generalised expected ductility values, μ_p, at ULS.

Description	Part ductility, μ_p
All rigid parts or components	N/A
Flexible parts or components	
with good post-yield deformation capacity	2.5
with unknown post-yield behaviour, but some expected inelastic displacement capacity or ability to slip or rock	1.5
with unknown post-yield behaviour that may be brittle	1.25

OPTIONAL PROVISIONS FOR LONG-PERIOD PARTS AND COMPONENTS

When the periods of the parts or components are much greater than those of the modes of building, the peak demands on the parts are correlated closely with those expected at the ground level, especially as the period of the part becomes greater. At these long periods, the relative motion from the modal response of the structure is not significantly influencing the response of the part. There is, however, a transition between parts with periods that are near the fundamental structural mode, where parts exhibit responses that are primarily determined from the modal response of the structure, to parts that exhibit responses that are well approximated using the corresponding ground response spectrum.

It is recommended that long-period parts and components should be defined as those possessing a period, T_p, that is greater than the threshold long period, $T_{p,long}$, which may be determined using Equation 8:

$$T_{p,long} = T_1(1+\sqrt{\mu}) \tag{8}$$

The threshold long period is equal to twice the fundamental structural period, T_1, when the structure is expected to respond elastically (i.e.: μ of 1.0). Structural nonlinearity has been widely observed to result in the lengthening of the structural modal periods [16; 19; 20; 22] and can effectively produce a plateau of demands between the initial elastic and the elongated inelastic periods [6; 83]. Existing floor response spectrum prediction approaches often limit the influence of period elongation to the demands associated with the fundamental structural mode, approximating the elongation by a factor of the square-root of the structural ductility [6; 11; 21], based on work by Priestley [84]. This has been observed to be conservative by other studies, which examined effective elongation fundamental periods on spectral demands [19; 22] and hence the form adopted in Equation 8 is recommended. Further, $T_{p,long} need not be taken less than 0.8\ s$.

If parts are found to have a period greater than the threshold long period using Equation 8, it is recommended that the design response coefficient, $C_p(T_p)$, be determined using Equation 9:

$$C_{p,long}(T_p) = \frac{S_a(T_p)}{C_{ph}}\left[1+\frac{1}{\left(\frac{T_p}{T_1}-1\right)^2}\right] \tag{9}$$

where $S_a(T_p)$ is determined from the seismic hazard at the con-

Table 6: Recommended classification and design ductility values of common parts or components.

Description of part or component	Class	Part effective ductility at ULS, μ_p	Supporting literature
Ceilings			[47; 49–53]
Direct fixed to underside of structural floors	Rigid	N/A	
Framed plasterboard ceilings	Flexible	2	
Suspended tile ceilings – braced (without vertical clips or similar to mitigate vertical dislodgement of ceiling tiles)	Flexible	1.5	
Suspended - unbraced	Flexible	N/A	
Suspended tile ceilings with clips (or similar) to mitigate vertical dislodgement of ceiling tiles.	Flexible	2	
Pre-cast Reinforced Concrete Cladding Panels (out-of-plane loading)	Flexible	2	[54–58]
Glass Façades, Balustrades and Walls (out-of-plane loading)			[59]
Framing systems supporting glazing, or structural glazing systems using laminated glass and multiple support points	Flexible	1.5	
Other structural glazing systems and individual glass panes	Flexible	1	
Timber-Framed Partitions, Façades, Balustrades and Walls (out-of-plane loading)	Flexible	2.5	[60; 61]
Masonry Façades, Parapets and Walls (out-of-plane loading)	Flexible	1.25	[62; 63]
Steel Framed Partitions, Façades and Parapet Walls (out-of-plane loading)	Flexible	2.5	[64]
Stairs (fixed to one level and free to slide at other)			[65–67]
Reinforced concrete, steel or timber Stairs	Flexible	2.5	
Storage Racks			[68–71]
Floor supported	Flexible	1.5	
Braced laterally top and bottom	Flexible	2	
Lifts and Guiderails	Flexible	2	[72–74]
Mechanical Parts or Components			[75–78]
Heavy equipment direct fixed to slabs or with saddle supports	Rigid	N/A	
Vibration isolated heavy equipment or HVAC equipment	Flexible	1.5	
Heavy equipment with other supports	Flexible	2	
Suspended equipment	Flexible	1.5	
Storage vessels (without hazardous materials)	Flexible	1.5	
HVAC equipment with stiff restraints	Flexible	2	
Distribution Systems			[48; 79]
Pipes	Flexible	1.5	
Ducts, conduits, and cable trays	Flexible	2	
Electrical Parts or Components			[80–82]
Lighting – surface mounted to underside of structural floors	Rigid	N/A	
Lighting – integrated within ceiling or stiff/braced pendant lighting	Flexible	1.5	
Electrical cabinets/equipment – fixed to structural floor	Flexible	2	
Electrical cabinets/equipment – fixed to walls or other parts	Flexible	1.5	
Heavy electrical equipment (e.g. transformers) direct fixed to slabs	Rigid	N/A	
Cantilever Structures and Penthouse Structures			
Capacity designed	Flexible	2.5	
Non-capacity designed	Flexible	1.25	
Raised Floors	Flexible	1.5	
Parts Supporting or Containing Hazardous Materials	Flexible	1	

sidered design level intensity in TS1170.5, and C_{ph} is the part response factor. The expression within the square brackets accounts for the transition between parts with periods that are near the fundamental structural mode which exhibit responses that are primarily determined from the modal response of the structure, to parts that exhibit responses that are well approximated using the corresponding ground response spectrum, and follows the expression for the long-period dynamic amplification factor in the modal superposition approach by Haymes et al. [43]. Similar expressions have been used in other modal approaches [20; 21].

Figure 2 demonstrates the application of the long-period part provisions using the UC Physics building example. Significant reduction in design loads may be achieved by applying this approach compared with the flexible parts provisions, particularly if the part is permitted to develop a ductile response. It is recognised that this may only apply to a limited number of parts that are characterised by long periods. However, if an engineer is prepared to compute the period of the part, then it can be seen that large reductions in strength requirements may result. This will most likely be applicable in buildings that are either short, stiff, or both, with short fundamental periods. Example applications for structural nonlinearity are provided later in this paper, requiring the consideration of period elongation. Further discussion can be found in [27].

PART RESERVE STRENGTH CAPACITY AND UPPER BOUND OF HORIZONTAL DESIGN FORCE

Part Reserve-Capacity Factor

As the majority of parts and components possess some ductility, and the total load required to reach failure will be higher than the nominal strength, the required yield strength for design should be set to the strength that ensures that deformation limits are not exceeded and thus the part capacity should consider the expected resistance at the limit state considered. Other international codes include an analogous factor to account for this behaviour, such the $q_{ap,S}$ behaviour factor of 1.3 in Eurocode 8, and the component strength factor R_{po} of 1.3 to 2.0 in ASCE 7-22. This is accounted for in the proposed recommendations by specifying the part reserve-capacity factor, Ω_p, set to 1.0 at SLS1, 1.25 at SLS2, and 1.5 at ULS, which is used to compute the recommended horizontal design earthquake action on a part, F_{ph}, in Equation 1. Ω_p should be taken as 1.0 for brittle parts. This parameter describes the ratio of the lateral strength (resistance) of the part or component at the limit state failure compared to the design value of resistance.

Basis of the Upper Bound of the Design Force

The horizontal design earthquake actions on a part normalised by the weight of the part, F_{ph}/W_p, determined Equation 1, has a upper bound of 7.5 PGA/Ω_p. This is derived considering a flexible part with unknown and potentially brittle behaviour, corresponding to a part spectral-shape coefficient, $C_i(T_p)$ of 4.0, and part response factor, C_{ph}, of 1.4, mounted at the roof of an elastic building with a short or unknown fundamental period, corresponding to a floor-height coefficient, C_{Hi}, of 3.5 and structural-nonlinearity-reduction factor, C_{str}, of 1.3. These values correspond to a design response coefficient for parts and components, $C_p(T_p)$, of 7.69PGA, which has been rounded to $7.5PGA/\Omega_p$. For the ultimate limit state (ULS), this then leads to a limit of 5PGA.

The ratio of the elastic 5%-damped roof level spectral accelerations of the considered New Zealand instrumented buildings to the corresponding peak ground acceleration, for part periods normalised by the buildings fundamental period, is given in Figure 10, similar to that presented in the ATC-120 report [16]. This figure shows that if a part or component is near resonance with the fundamental structural modal period, significant dynamic amplification may occur, generating strength demands above 7.5PGA. However, if the period of the part falls further from the fundamental period, here shown with bounds at 15% and 25%, the amplification significantly lessens. The limit of $7.5PGA/\Omega_p$ for all components has been set considering that even though it could be used for very brittle components or for low intensities where a part ductility of 1.25 is not permitted, there is also a good chance that such components, if present, may not exhibit a period similar to the fundamental modal period of the supporting structure. Consider also that while the 2004 New Zealand loadings standard NZS 1170.5 limits the horizontal design force acting on parts and components to the weight of the part, W_p, factored by 3.6, there does not appear to be a robust scientific basis for this limit. It should also be noted that the peak force that different parts on a floor need to resist are not expected to be experienced by all parts contemporarily. Thus, structural floor systems should still be designed for loads associated with a suitable consideration of total inertia actions on the floors.

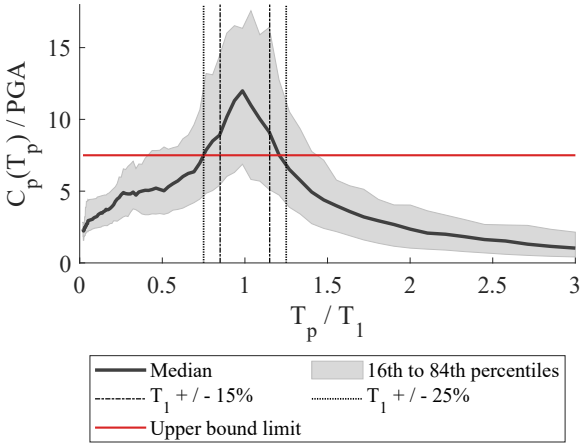

Figure 10: Ratio of the roof level spectral accelerations in New Zealand instrumented buildings to the corresponding peak ground acceleration, for part periods normalised by T_1. The proposed upper bound is indicated.

Unlike ASCE 7-22, NZS 1170.5 does not currently have a lower bound for the horizontal design force and is not recommended, as no strong rationale was found here.

COMPARATIVE APPLICATION WITH INTERNATIONAL CODE APPROACHES

The performance of the recommended approach, the existing NZS 1170.5 parts approach, and those provided in the new ASCE 7-22 and Eurocode 8 codes, are examined here using the time-history analysis results from the eight-storey RC wall and steel MRF buildings. Earthquake motions that resulted in structural ductility values within 15% of 1.0, 2.0, and 4.0 are examined for both buildings. While it is difficult to apply international code approaches consistently because of unique approaches for defining ground motion intensity, the comparisons provided here are made relative to the peak ground acceleration, PGA, for the sake of providing an approximation of the relative predictive performance of the code approaches. The modal properties of the considered structures, for use in the Eurocode 8 approach, were adopted from Welch [32].

Figure 11 shows the median and sixteenth to eighty-fourth percentile distribution of the ground response spectra, normalised by PGA, for all considered motions in each building. The modal pe-

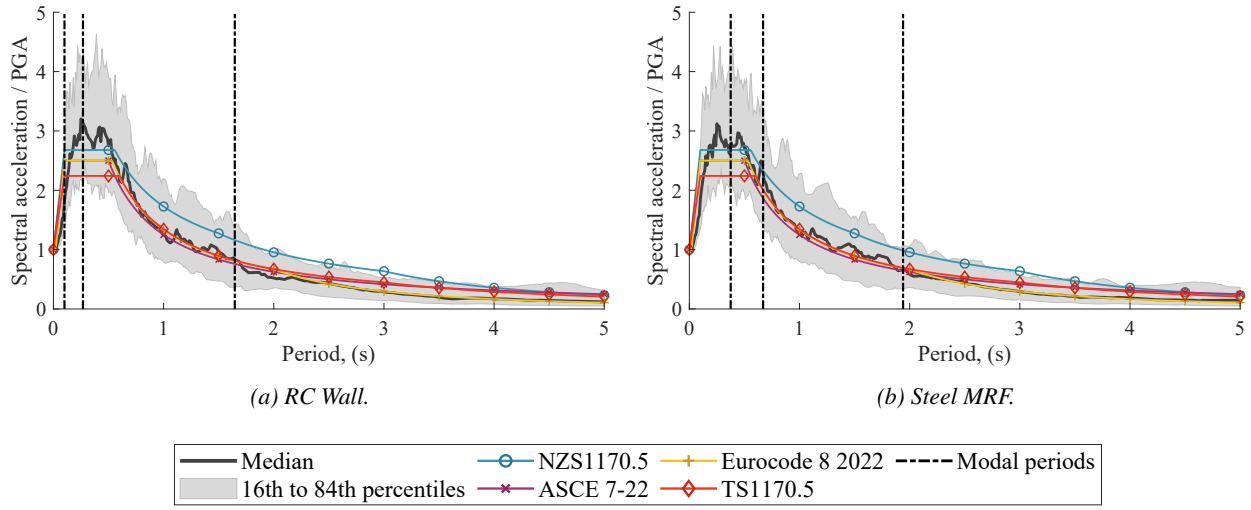

(a) RC Wall. *(b) Steel MRF.*

Figure 11: Median and sixteenth to eighty-fourth percentile distribution of the ground response spectra, normalised by PGA, for all considered motions in each building. The code design ground response spectra considered here are shown, and the modal periods of each structure are indicated.

riods of each structure are indicated. The design ground response spectrum shapes of the four code approaches are overlaid, and were selected to approximate the median time-history ground spectrum curves. The NZS 1170.5 design ground response spectrum was constructed using soil class D. The TS1170.5 design ground response spectrum was constructed approximating the motions considering an annual probability of exceedance of one-in-250 in Christchurch on site class V. The ASCE 7-22 design ground response spectrum was constructed using the non-site specific two period design spectrum approach. It was approximated that the short period spectral acceleration, S_{DS}, is $2.5PGA$. Although not used in the part approach, the shape shown in the figure was constructed using a long period T_L of 8.0 s, and assuming that the spectral acceleration at one second, S_{D1}, is $0.5S_{DS}$. The Eurocode 8 2022 design ground response spectrum was constructed considering a class B soil in a high seismicity area, with an f_h of 0.4, an χ value of 4.0, and assuming that the short period spectral acceleration, F_A, is $2.5PGA$.

Beyond the comparisons provided here, work by Haymes and Sullivan [27] gives further comparisons for a range of hypothetical buildings and design applications using the current NZS 1170.5 parts approach considering the ground motion intensities characterised in NZS 1170.5 and new national seismic hazard model (NSHM), as well as the recommended approach using the NSHM. The appendix to the current work also provides worked examples of some common design applications of the recommended approach.

Demands on Rigid Components Described By Peak Floor Accelerations

Figure 12 compares the prediction of peak floor acceleration, *PFA*, demands for the eight-storey RC wall and steel MRF structures at three structural ductility values, normalised by the peak ground acceleration, *PGA*, using the various code approaches and the new New Zealand recommendations. The predictions are shown as a function of floor height normalised by the total building height (h_i / h_n). Demands at floors two, four, six, and eight are shown. The predictions overlay the median and sixteenth to eighty-fourth percentile distribution of the time-history results. The Eurocode 8 'simple' approach denotes the simplified expression given in Equation 7.3 of Eurocode 8 2022, whereas 'modal' denotes the peak floor accelerations predicted using the modal superposition approach in Annex C of Eurocode 8.

The European and American code approaches account for structural nonlinearity using tables that set values for effective reduction factors, analogous to C_{str}, in their design codes based on structural typology for the one design limit state considered in each code. The present work applies all considered approaches at three structural ductility values, and thereby required assumptions and approximations which may not strictly follow the code intent. The Eurocode 8 approaches were applied by approximating the building behaviour factor (force reduction factor to account for deformation capacity and energy dissipation capacity), q_D, as being equal to the structural ductility value, as in the work by Vukobratovic and Fajfar [20] from which the Eurocode 8 approach appears to be derived. The application of the ASCE 7-22 approach also set the structure ductility reduction factor, R_μ, equal to structural ductility, as in the ATC-120 report [16].

The peak floor acceleration estimated using NZS 1170.5 are seen to produce highly conservative estimates of the *PFA*/*PGA* distribution using the NZS 1170.5 C_{Hi}, which are significantly greater than most other applications of the other approaches. In fact, the theoretical design demands on floors and rigid parts would be as high as twice these estimates because NZS 1170.5 amplifies C_{Hi} by 2.0 using the NZS 1170.5 $C_i(T_p)$ for parts with periods shorter than 0.75 s. NZS 1170.5 does allow these estimates to be reduced with part ductility using C_{ph}, although this would still result in highly conservative estimates. Even if very ductile parts are considered ($\mu_p \geq 3$), the NZS 1170.5 approach would produce estimates equal to 90% of the demands shown in Figure 12.

The simple Eurocode 8 approach similarly produces very conservative estimates in the upper floors when the structure responded elastically. The simple Eurocode 8 predictions over lower floors rely heavily on the lower limit of the approach, that *PFA* is equal to or greater than *PGA*, to produce reasonable, although sometimes conservative, estimates. ASCE 7-22 similarly applies a lower bound, equivalent to $0.75PGA$, which governed over lower levels. This appears to be non-conservative in the lower half of the RC wall building, thought to be due to the application of the structure ductility reduction factor, R_μ, being applied at the same magnitude over all floors. The approach recommended here for New Zealand produces identical estimates to the ASCE 7-22 approach at the roof level, differing only in the shape of the structural-nonlinearity-reduction factor, altered by including e_{str}, which appears to produce more accurate estimates over all floors

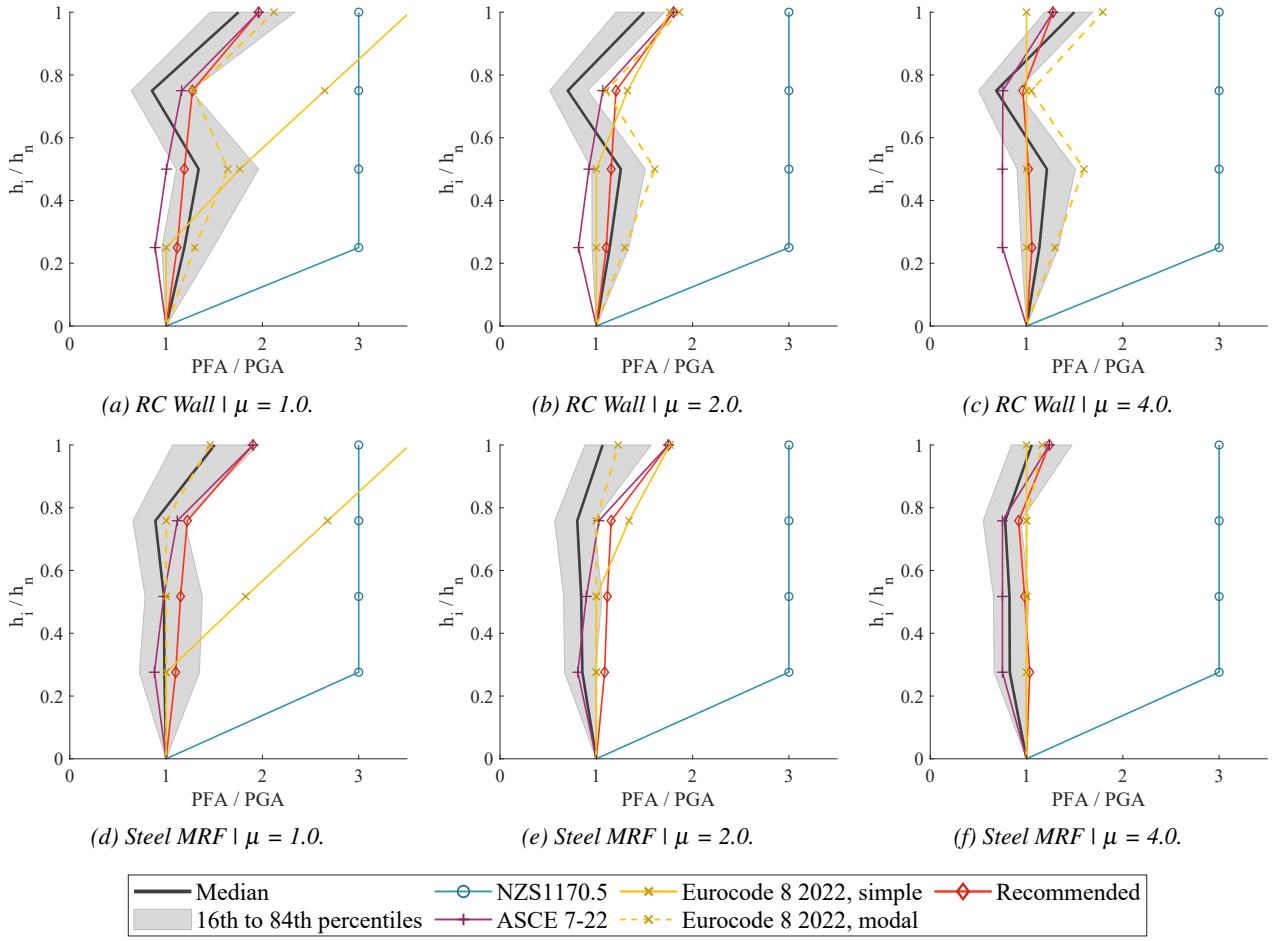

Figure 12: Prediction of peak floor acceleration (PFA) demands for the eight-storey RC wall and steel MRF structures at three structural ductility values, normalised by the peak ground acceleration (PGA), using the recommended and code approaches, as a function of floor height, normalised by the total building height (h_i / h_n). The median and sixteenth to eighty-fourth percentile distribution of the time-history results are indicated.

without depending on a lower bound.

The *PFA*/*PGA* distribution in the RC wall building exhibits an "S" shape, with large amplification near the mid-height and roof, with lower demands at floor six of the eight total. The steel MRF building, conversely, exhibits a distribution closer to the hook-shape assumed by the ASCE 7-22 and recommended floor-height coefficients. This is likely due to significant higher mode response in the RC wall buildings that are not reduced significantly by the formation of the plastic hinge at the base of the structure, whereas plasticity occurs throughout the MRF. The Eurocode 8 modal approach appears to produce the most reliable predictions in both buildings, with most predicted values between the fiftieth and eighty-fourth percentiles. Although this approach is able to achieve greater accuracy, it requires more computational effort and more specific information about the buildings, the mode shapes and periods of the structure. This trade-off is fundamental to the development of practice-oriented methods, and the recommended approach has opted to maintain a greater ease of use, in-line with perspectives expressed by industry during a workshop held in 2022 [27].

Demands on Flexible Components Described By Floor Response Spectra

Figures 13 and 14 show predictions of design response coefficient for parts and components, $C_p(T_p)$, normalised by the peak ground acceleration (PGA), using the recommended and code approaches for the roof level of the eight-storey RC wall and steel MRF structures, respectively. The design response coefficient for parts and components represents the part yield strength required to ensure a given part ductility capacity is not exceeded. The coefficient is given as a function of the period of the part (i.e.: a design spectrum), normalised by the ratio of the peak ground acceleration and the weight of the part, PGA/W_p. Spectra were produced for structural ductility values of 1.0, 2.0, and 4.0; and the part ductility values of 1.0 and 2.0. The median and sixteenth to eighty-fourth percentile distribution of the time-history results are indicated. The recommended approach was applied for rigid, flexible and long-period parts, and the threshold long period, $T_{p,long}$, is shown.

The recommended approach does not require engineers to estimate the periods of the part nor building, as desired by industry [27], and therefore relies only on the rigid/flexible classification. Consequently, the recommended approach attempts to manage the risk of the part experiencing significant demands due to proximity of the part and structural modal periods, assuming that parts with periods above 0.06 s may experience significant dynamic amplification. The demands computed using time-history analysis in Figures 13 and 14 appear to infrequently exceed the values predicted by the recommended approach. Although this results in estimates that are conservative for many part periods, the degree that estimates are conservative generally remains proportional to the highest observed spectral demands with the varying structural and part ductility values.

The ASCE 7-22 approach appears to apply a similar rigid/flexible

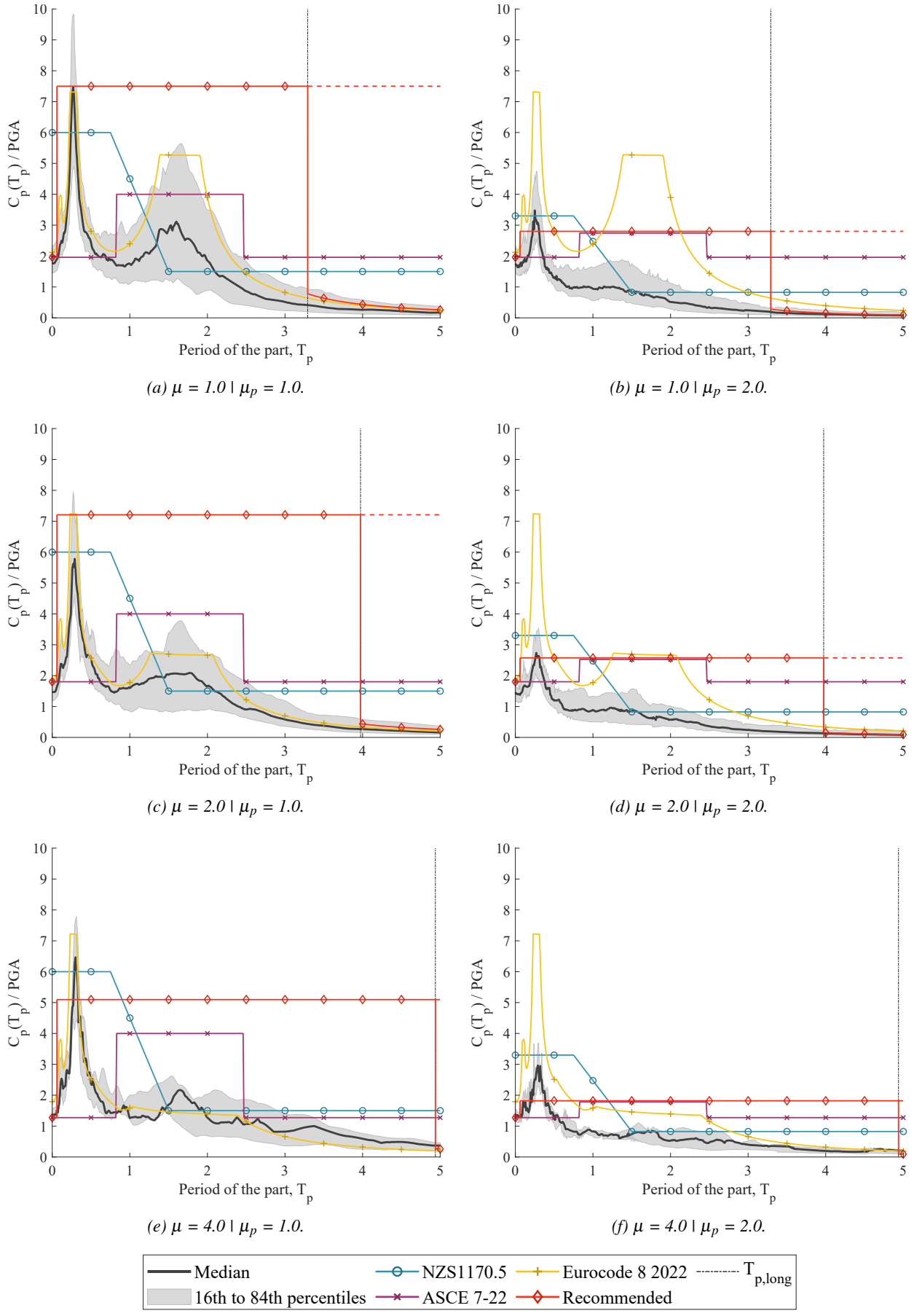

Figure 13: Predictions of the design response coefficient for parts and components, $C_p(T_p)$, for the roof level of the eight-storey RC wall structure at three structural ductility values, normalised by the peak ground acceleration (PGA), using the recommended and code approaches. Predictions overlay the median and sixteenth to eighty-fourth percentile distribution of the time-history results.

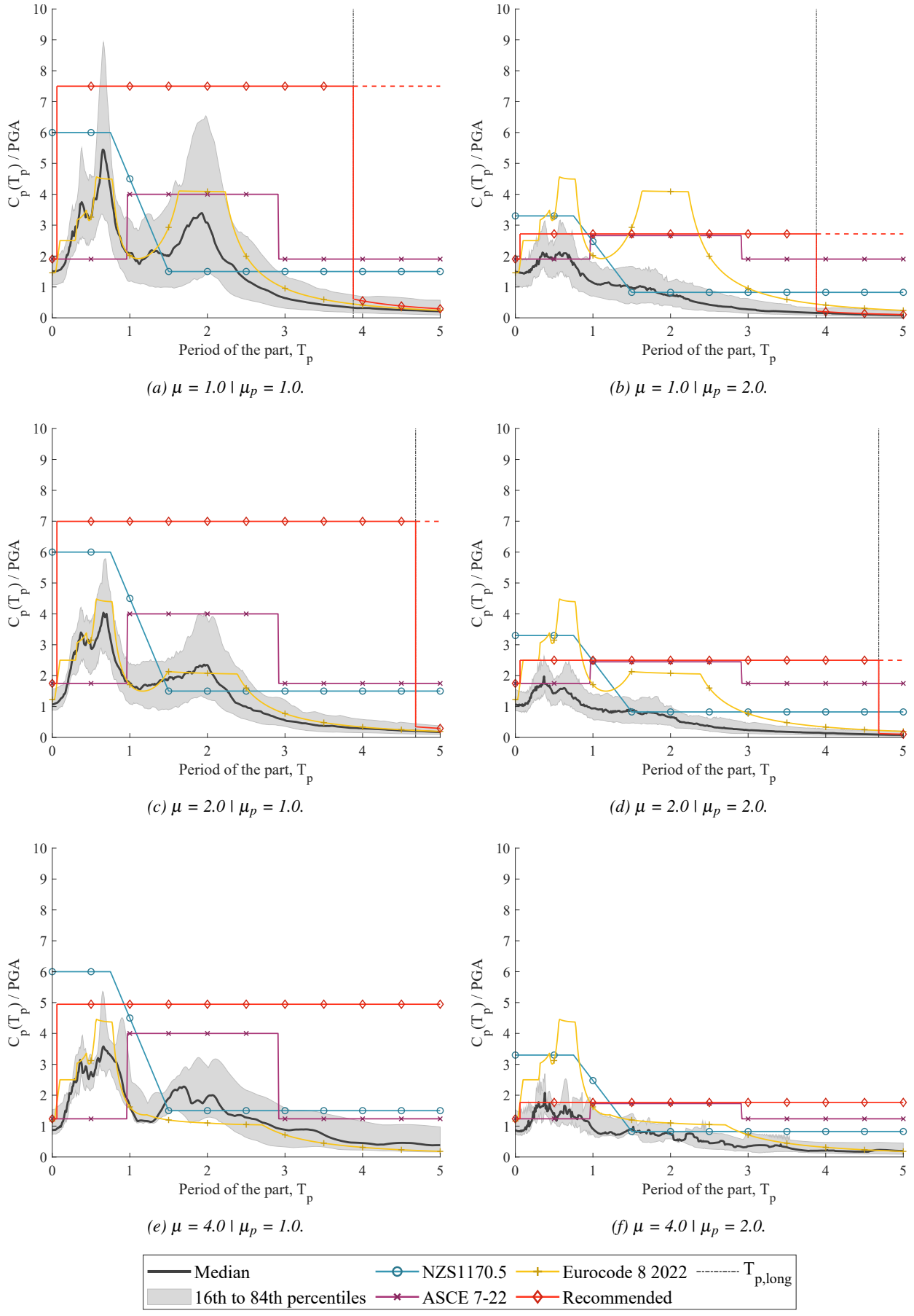

Figure 14: Predictions of the design response coefficient for parts and components, $C_p(T_p)$, for the roof level of the eight-storey steel MRF structure at three structural ductility values, normalised by the peak ground acceleration (PGA), using the recommended and code approaches. Predictions overlay the median and sixteenth to eighty-fourth percentile distribution of the time-history results.

classification approach in the tabulated values for the component resonance ductility factor, C_{AR}, but specifies that a component is likely to be in resonance with the structure if the period of the part is between 0.5 to 1.5 of fundamental structural period. This fails to describe the significant amplifications associated with higher modal response, near 0.2 s for the RC wall building and between 0.25 s and 0.75 s in the steel MRF buildings. The ASCE 7-22 upper bound of 4.0*PGA* applies for many structure ductility values for parts with limited ductility and periods near the fundamental structural period.

The NZS 1170.5 spectral-shape coefficient produces more conservative estimates of the demands on ductile parts with relatively short periods, less than 0.75 s, which, as in these examples, may be influenced by higher mode structural response. A building with fundamental period, T_1, greater than 0.75 s, as in these example structures, is likely to exhibit floor response spectra that are well described by the NZS 1170.5 spectral shape when the structure, but not the part, has developed significant nonlinearity, producing significant reductions in the demands associated with the fundamental modal response of the structure. Indeed, the NZS 1170.5 predictions are most similar to the spectra computed from the time-history results in Figures 13e and 14e, where μ is 4.0 and μ_p is 1.0. Consequently, when T_1 is greater than 0.75 s, the NZS 1170.5 spectral shape may be non-conservative if neither the part nor the structure is not permitted to respond nonlinearly, such as at the serviceability limit state, resulting in the significant amplification of demands for parts with periods near the T_1, as demonstrated in Figure 8. The NZS 1170.5 approach appears overly conservative when both the structure and part are permitted to develop ductility, however, and the recommended approach can produce lower estimates that appear to better reflect the beneficial reductions that both forms of nonlinearity may provide.

The Eurocode 8 modal superposition approach is able to produce highly accurate and specific predictions of the amplified demands associated with the first three structural modes, as well as the behaviour of long-period parts when the part remains elastic (μ_p of 1.0). However, the Eurocode 8 modal approach results in conservative estimates when the part develops ductility (μ_p of 2.0). The Eurocode 8 approach does not fully describe the beneficial reductions due to ductile part response because the frequency-dependent behaviour factor component accounting for the deformation capacity and energy dissipation capacity of the part, $q_{ap,D}$ is taken as 2.0 for all elements that are permitted to dissipate energy by inelastic deformation. Consider also that Eurocode 8 requires the use of a 2% part damping value unless demonstrated to be greater. The spectra shown in Figures 13 and 14 were computed a 5% part damping value, and it is expected that common design applications will therefore lead to greater design strength requirements.

The provisions for long-period parts appears to produce reliable estimates of the median spectra computed from the time-history results, reducing proportionally to the part ductility values. The threshold long period, $T_{p,long}$, is very long for these structures, especially when the elongation of the fundamental structural period is considered, and it is thought unlikely that many parts will demonstrate such long periods. This approach will therefore have greater applicability for short and stiff buildings. Future research could look to reduce the $T_{p,long}$ limit (Equation 8).

CONCLUSIONS

This work recommends revisions to Section 8 Requirements for Parts and Components of the New Zealand Standard NZS 1170.5:2004 Structural Design Actions, Part 5: Earthquake Actions. The recommendations were developed considering the latest international literature and perceptions expressed during a recent workshop attended by New Zealand engineering practitioners and academics as well as within the New Zealand Seismic Risk Working Group (SRWG). Parameters were refined and introduced considering the existing framework of the design standard where possible to help facilitate adoption.

The approach was developed considering the uncertainties and difficulties in the characterisation of many parameters, such as the modal period(s), ductility, and damping of the part and the structure. The recommended approach may be applied considering only simple parameters and providing guidance where needed to maintain the ease of use.

One significant change recommended is for the prediction of peak floor accelerations via the floor-height coefficient, C_{Hi}. The approach set out in ASCE 7-22, which was checked against a large set of instrumented buildings, is recommended for use in New Zealand and will lead to lower part strength requirements.

The new recommended approach also introduces a structural-nonlinearity-reduction factor, C_{str}, which accounts for the beneficial reduction in peak floor accelerations that have been widely observed to occur due to structural nonlinearity, developed through material inelasticity or geometric nonlinearity. However, the recommended approach differs from ASCE 7-22 by also considering the reduction as a function of floor height. This will lead to lower part strength requirements than those produced using NZS 1170.5.

One of the main simplifications is to allow parts to be designed without evaluating their period of vibration. This lead to the classification of parts as either rigid or flexible to manage the risk of the part experiencing significant demands due to proximity of the part and structural modal periods, assuming that parts with periods above 0.06 s may experience significant dynamic amplification of the part response relative to the peak floor acceleration using the part or component spectral-shape coefficient, $C_i(T_p)$. The rigid/flexible classification further used to refine the part-response or component-response factor, C_{ph}, to reliably estimate the beneficial reductions in part strength requirements than can be achieved for ductile flexible parts. These parameters will result in reduced part strength requirements for rigid components, but will lead to increased part strength requirements for flexible parts that are not permitted to develop ductile responses at the considered design limit state.

The estimates produced by the recommended and existing code approaches for rigid and flexible parts were compared using case study examples to demonstrate that the revisions may be adopted without resulting in significantly increased loading in many applications. It was illustrated that increased demand estimates may only result from the application of the recommended approach for flexible parts with limited ductile capacity, and for some parts at the serviceability limit state design level. Conversely, this study demonstrated that lower design part strength requirements can be achieved for applications where the NZS 1170.5 approach was considered to be overly conservative. This includes rigid parts; parts on lower levels of buildings; ductile flexible parts; parts in ductile buildings at the ultimate limit state design; and parts with sufficiently long periods.

The most recent updates to the code design approaches in Europe and the United States were compared to the recommended and NZS 1170.5 design approaches for parts. Although adopting similar provisions to ASCE 7-22, the recommended approach was observed to produce estimates closer to observed demands at short periods and the lower levels of the structure by considering higher mode response and the distribution of reductions due to structural nonlinearity with floor height. The Eurocode 8

modal superposition approach was found to produce the most accurate results for most design applications, but required more building information and computational expenditure which was not thought feasible in practice by workshop participants.

ACKNOWLEDGEMENTS

The authors would like to acknowledge the contributions and direction provided by the Seismic Risk Working Group under Engineering New Zealand. This project was also informed by the perspectives and opinions of the practitioners and researchers that attended a workshop held at the University of Canterbury in June 2022. Their invaluable contributions are recognised.

This project was partially supported by QuakeCoRE, a New Zealand Tertiary Education Commission-funded Centre. This is QuakeCoRE publication number 914. The research has also been supported by the Resilience to Nature's Challenges project, and the New Zealand Earthquake Commission, Toka Tū Ake EQC. Their support is gratefully acknowledged.

REFERENCES

1 Standards New Zealand (2016). *NZS 1170.5:2004: Structural design actions, Part 5: Earthquake actions - New Zealand*. Standards New Zealand, Wellington, New Zealand.

2 Chandramohan R, Ma Q, Wotherspoon LM, Bradley BA, Nayyerloo M, Uma SR and Stephens MT (2017). "Response of instrumented buildings under the 2016 Kaikoura earthquake". *Bulletin of the New Zealand Society for Earthquake Engineering*, **50**(2): 237–252. https://doi.org/10.5459/bnzsee.50.2.237-252

3 Dhakal RP, Pourali A, Tasligedik AS, Yeow T, Baird A, MacRae G, Pampanin S and Palermo A (2016). "Seismic performance of non-structural components and contents in buildings: an overview of NZ research". *Earthquake Engineering and Engineering Vibration*, **15**(1): 1–17. https://doi.org/0.1007/s11803-016-0301-9

4 Khakurel S, Dhakal RP, Yeow TZ and Saha SK (2020). "Performance group weighting factors for rapid seismic loss estimation of buildings of different usage". *Earthquake Spectra*: 875529301990131. https://doi.org/10.1177/8755293019901311

5 Stanway JM (2022). "Seismic Performance of Non-Structural Elements in New Zealand – What have we learnt?" *Fifth International Workshop on the Seismic Performance of Non-Structural Elements (SPONSE)*, Stanford University, California, USA.

6 Sullivan TJ, Calvi PM and Nascimbene R (2013). "Towards improved floor spectra estimates for seismic design". *Earthquakes and Structures*, **4**(1): 109–132. https://doi.org/10.12989/eas.2013.4.1.109

7 Biggs J (1971). "Seismic response spectra for equipment design in nuclear power plants". *First International Conference on "Structural Mechanics in Reactor Technology"*, Berlin, Germany, pp. 329–343.

8 Kelly TE (1978). "Floor response of yielding structures". *Bulletin of the New Zealand Society for Earthquake Engineering*, **11**(4): 255–272. https://doi.org/10.5459/bnzsee.11.4.255-272

9 Taghavi S and Miranda E (2008). "Effect of interaction between primary and secondary systems on in-structure response spectra". *14th World Conference on Earthquake Engineering*, Beijing, China, pp. 12–17.

10 Calvi PM (2014). "Relative Displacement Floor Spectra for Seismic Design of Non Structural Elements". *Journal of Earthquake Engineering*, **18**: 1037–1059. https://doi.org/10.1080/13632469.2014.923795

11 Filiatrault A and Sullivan T (2014). "Performance-based seismic design of nonstructural building components: The next frontier of earthquake engineering". *Earthquake Engineering and Engineering Vibration*, **13**(S1): 17–46. https://doi.org/10.1007/s11803-014-0238-9

12 Lucchini A, Franchin P and Mollaioli F (2016). "Probabilistic seismic demand model for nonstructural components". *Earthquake Engineering & Structural Dynamics*, **45**(4): 599–617. https://doi.org/10.1002/eqe.2674

13 Miranda E, Kazantzi A and Vamvatsikos D (2018). "New approach to the design of acceleration-sensitive non-structural elements in buildings". *16th European Conference on Earthquake Engineering*, Thessaloniki, Greece.

14 Merino RJ, Perrone D and Filiatrault A (2020). "Consistent floor response spectra for performance-based seismic design of nonstructural elements". *Earthquake Engineering & Structural Dynamics*, **49**: 261–284. https://doi.org/10.1002/eqe.3236

15 Kazantzi AK, Miranda E and Vamvatsikos D (2020). "Strength-reduction factors for the design of light nonstructural elements in buildings". *Earthquake Engineering & Structural Dynamics*. https://doi.org/10.1002/eqe.3292

16 Applied Technology Council (2018). *Recommendations for improved seismic performance of nonstructural components*. Tech. rep., National Institute of Standards and Technology, Redwood City. https://doi.org/10.6028/NIST.GCR.18-917-43

17 Shelton RH (2004). *Seismic response of building parts and non-structural components*. Tech. rep., BRANZ.

18 Kehoe BE and Hachem M (2003). "Procedures for Estimating Floor Accelerations". *ATC-29-2 Seminar on Seismic Design, Performance, and Retrofit of Nonstructural Components in Critical Facilities*, Applied Technology Council, Redwood City, California, USA.

19 Calvi PM and Sullivan TJ (2014). "Estimating floor spectra in multiple degree of freedom systems". *Earthquakes and Structures*, **7**(1): 17–38. https://doi.org/10.12989/eas.2014.7.1.017

20 Vukobratović V and Fajfar P (2017). "Code-oriented floor acceleration spectra for building structures". *Bulletin of Earthquake Engineering*, **15**(7): 3013–3026. https://doi.org/10.1007/s10518-016-0076-4

21 Welch DP and Sullivan TJ (2017). "Illustrating a new possibility for the estimation of floor spectra in nonlinear multi-degree of freedom systems". *16th World Conference on Earthquake Engineering*, Paper 2632, Santiago, Chile.

22 Haymes K (2023). "Developing Procedures for the Prediction of Floor Response Spectra, PhD Thesis, University of Canterbury".

23 American Society of Civil Engineers (2021). *ASCE/SEI 7-22 Minimum Design Loads and Associated Criteria for Buildings and Other Structures*. ISBN 9780784415788.

24 European Committee for Standardization (2004). "Eurocode 8: Design of structures for earthquake resistance - Part 1: General rules, seismic actions and rules for buildings".

25 Rashid M, Dhakal R and Sullivan T (2021). "Seismic design of acceleration-sensitive non-structural elements in New Zealand: State-of-practice and recommended changes". *Bulletin of the New Zealand Society for Earthquake Engineering*, **54**: 243–262. https://doi.org/10.5459/bnzsee.54.4.243-262

26 Uma SR, Zhao JX and King AB (2010). "Seismic actions on acceleration sensitive non-structural components in ductile frames". *Bulletin of the New Zealand Society for Earthquake Engineering*, **43**(2): 110–125. https://doi.org/10.5459/bnzsee.43.2.110-125

27 Haymes K and Sullivan T (2023). *Recommended Revisions to the Approach in NZS 1170.5:2004 for the Seismic Design of Parts and Components*. Tech. rep., University of Canterbury.

28 GeoNet (2023). "Structural Array Data". https://www.geonet.org.nz/data/types/structural_arrays

29 McHattie S (2013). *Seismic Response of the UC Physics Building in the Canterbury Earthquakes*. Master of engineering thesis, University of Canterbury.

30 Carr A (2006). "RUAUMOKO3D-Inelastic dynamic analysis program".

31 Federal Emergency Management Agency (FEMA) (2009). "FEMA P695: Recommended Methodology for Quantification of Building System Performance and Response Parameters. Project ATC-63".

32 Welch DP (2016). *Non-structural element considerations for contemporary performance-based earthquake engineering*. Phd thesis, Scuola Universitaria Superiore IUSS Pavia.

33 Feinstein T and Moehle JP (2022). "Seismic response of floor-anchored nonstructural components fastened with yielding elements". *Earthquake Engineering & Structural Dynamics*, **51**: 3–21. https://doi.org/10.1002/eqe.3553

34 Miranda E and Taghavi S (2009). "A Comprehensive Study of Floor Acceleration Demands in Multi-Story Buildings". American Society of Civil Engineers, Reston, VA, USA, ISBN 9780784410844, pp. 616–626. https://doi.org/10.1061/41084(364)57

35 Drake RM and Bachman RE (1995). "Interpretation of instrumented building seismic data and implications for building codes". *Structural Engineers Association of California Conference*, California, USA.

36 Fathali S and Lizundia B (2011). "Evaluation of current seismic design equations for nonstructural components in tall buildings using strong motion records". *The Structural Design of Tall and Special Buildings*, **20**: 30–46, doi: 10.1002/tal.736. https://doi.org/10.1002/tal.736

37 Standards New Zealand (2016). "NZS 1170.5 Supp 1:2004 Structural design actions - Part 5: Earthquake actions - New Zealand Commentary".

38 Sullivan TJ, Priestley MJN and Calvi GM (2008). "Estimating the Higher-Mode Response of Ductile Structures". *Journal of Earthquake Engineering*, **12**: 456–472. https://doi.org/10.1080/13632460701512399

39 Kazantzi A, Vamvatsikos D and Miranda E (2018). "Effect of yielding on the seismic demands of nonstructural elements". *16th European Conference on Earthquake Engineering*, Thessaloniki, Greece.

40 Vukobratović V, Yeow TZ and Kusunoki K (2021). "Floor acceleration demands in three RC buildings subjected to multiple excitations during shake table tests". *Bulletin of Earthquake Engineering*, **19**: 5495–5523. https://doi.org/10.1007/s10518-021-01181-2

41 Adam C and Furtmüller T (2008). "Response of nonstructural components in ductile load-bearing structures subjected to ordinary ground motions". *14th World Conference on Earthquake Engineering*, Beijing, China.

42 Rodriguez ME, Restrepo JI and Carr AJ (2002). "Earthquake-induced floor horizontal accelerations in buildings". *Earthquake Engineering & Structural Dynamics*, **31**(3): 693–718. https://doi.org/10.1002/eqe.149

43 Haymes K, Sullivan T and Chandramohan R (2020). "A practice-oriented method for estimating elastic floor response spectra". *Bulletin of the New Zealand Society for Earthquake Engineering*, **53**: 116–136. https://doi.org/10.5459/bnzsee.53.3.116-136

44 Kehoe BE (2014). "Defining rigid vs. flexible nonstructural components". *10th U.S. National Conference on Earthquake Engineering*, Anchorage, AK, USA.

45 Watkins D, Chui L, Hutchinson T and Hoehler M (2010). *Survey and Characterisation of Floor and Wall Mounted Mechanical and Electrical Equipment in Buildings. Report No. SSRP-2009/11*. Tech. rep., Department of Structural Engineering, University of California, San Diego.

46 Marsantyo R, Shimazu T and Araki H (2000). "Dynamic response of nonstructural systems mounted on floors of buildings". *12th World Conference on Earthquake Engineering*, Auckland, New Zealand.

47 Ryu KP, Reinhorn AM and Filiatrault A (2012). "Full scale dynamic testing of large area suspended ceiling system". *15th World Conference on Earthquake Engineering*, Lisbon, Portugal.

48 Tian Y, Filiatrault A and Mosqueda G (2015). "Seismic Response of Pressurized Fire Sprinkler Piping Systems I: Experimental Study". *Journal of Earthquake Engineering*, **19**(4): 649–673. https://doi.org/10.1080/13632469.2014.994147

49 Badillo-Almaraz H, Whittaker AS and Reinhorn AM (2007). "Seismic Fragility of Suspended Ceiling Systems". *Earthquake Spectra*, **23**: 21–40. https://doi.org/10.1193/1.2357626

50 Pourali A, P DR, MacRae GA and S TA (2015). "Shake table tests of perimeter-fixed type suspended ceilings". *New Zealand Society for Earthquake Engineering Conference 2015*, Rotorua, New Zealand.

51 Soroushian S, Maragakis EM and Jenkins C (2015). "Capacity Evaluation of Suspended Ceiling Components, Part 1: Experimental Studies". *Journal of Earthquake Engineering*, **19**: 784–804. https://doi.org/10.1080/13632469.2014.998354

52 Soroushian S, Rahmanishamsi E, Ryu KP, Maragakis M and Reinhorn AM (2016). "Experimental Fragility Analysis of Suspension Ceiling Systems". *Earthquake Spectra*, **32**: 881–908. https://doi.org/10.1193/071514eqs109m

53 Dhakal RP, MacRae GA, Pourali A and Paganotti G (2016). "Seismic fragility of suspended ceiling systems used in NZ based on component tests". *Bulletin of the New Zealand Society for Earthquake Engineering*, **49**: 45–63. https://doi.org/10.5459/bnzsee.49.1.45-63

54 Burley J, Faitotoa T, Seifi P, Henry RS and Ingham JM (2014). "Out-of-plane behaviour of connections between precast concrete panels and their foundations". *New Zealand Concrete Industry Conference 2014*, Taupo, New Zealand.

55 Belleri A, Cornali F, Passoni C, Marini A and Riva P (2018). "Evaluation of out-of-plane seismic performance of column-to-column precast concrete cladding panels in one-storey industrial buildings". *Earthquake Engineering Structural Dynamics*, **47**: 397–417. https://doi.org/10.1002/eqe.2956

56 McMullin KM, Ortiz M, Patel L, Yarra S, Kishimoto T, Stewart C and Steed B (2012). "Response of Exterior Precast Concrete Cladding Panels in NEES-TIPS/NEESGC/E-Defense Tests on a Full Scale 5-Story Building". *Structures Congress 2012*, American Society of Civil Engineers, Reston, VA, ISBN 9780784412367, pp. 1305–1314. https:

//doi.org/10.1061/9780784412367.117

57 Menichini G, Monte ED, Orlando M and Vignoli A (2020). "Out-of-plane capacity of cladding panel-to-structure connections in one-story R/C precast structures". *Bulletin of Earthquake Engineering*, **18**: 6849–6882. https://doi.org/10.1007/s10518-020-00962-5

58 Zoubek B, Fischinger M and Isaković T (2016). "Cyclic response of hammer-head strap cladding-to-structure connections used in RC precast building". *Engineering Structures*, **119**: 135–148. https://doi.org/10.1016/j.engstruct.2016.04.002

59 Galuppi L and Royer-Carfagni G (2018). "The post-breakage response of laminated heat-treated glass under in plane and out of plane loading". *Composites Part B: Engineering*, **147**: 227–239. https://doi.org/10.1016/j.compositesb.2018.04.005

60 Thurston SJ (2006). *Racking Tests on Rooms and Isolated Walls to Investigate Uplift Restraint and Systems Effects*. Tech. rep., BRANZ, New Zealand.

61 Bhatta J, Mulligan J, Dhakal RP, Sullivan TJ, Gerlich H and Kang F (2021). "Theoretical and experimental evaluation of timber-framed partitions under lateral drift". *Bulletin of the New Zealand Society for Earthquake Engineering*, **54**: 263–281. https://doi.org/10.5459/bnzsee.54.4.263-281

62 Dizhur D, Walsh K, Giongo I, Derakhshan H and Ingham J (2018). "Out-of-plane Proof Testing of Masonry Infill Walls". *Structures*, **15**: 244–258. https://doi.org/10.1016/j.istruc.2018.07.003

63 Griffith M and Vaculik J (2007). "Out-of-Plane Flexural Strength of Unreinforced Clay Brick Masonry Walls". *TMS Journal*, **25**: 53–68.

64 Mulligan J, Sullivan TJ and Dhakal RP (2022). "Experimental Seismic Performance of Partly-Sliding Partition Walls". *Journal of Earthquake Engineering*, **26**: 1630–1655. https://doi.org/10.1080/13632469.2020.1733139

65 Bull D (2011). "Stairs and Access Ramps between Floors in Multi-storey".

66 Higgins C (2009). "Prefabricated Steel Stair Performance under Combined Seismic and Gravity Loads". *Journal of Structural Engineering*, **135**: 122–129. https://doi.org/10.1061/(ASCE)0733-9445(2009)135:2(122)

67 Sorosh S, Hutchinson TC, Ryan K, Wichman K, Smith K, Belvin R and Berman JW (2022). "Numerical Simulation of Prefabricated Steel Stairs to be Implemented in the NHERI Tall Wood Building". *Fifth International Workshop on the Seismic Performance of Non-Structural Elements (SPONSE)*, Stanford University, California, USA.

68 López-Almansa F, Bové O, Casafont M, Ferrer M and Bonada J (2022). "State-of-the-art review on adjustable pallet racks testing for seismic design". *Thin-Walled Structures*, **181**: 110126. https://doi.org/10.1016/j.tws.2022.110126

69 Uma SR and Beattie G (2011). "Observed performance of industrial pallet rack storage systems in the Canterbury earthquakes". *Bulletin of the New Zealand Society for Earthquake Engineering*, **44**: 388–393. https://doi.org/10.5459/bnzsee.44.4.388-393

70 European Commission, Directorate-General for Research and Innovation (2016). *Seismic behaviour of steel storage pallet racking systems (SEISRACKS2) Final Report*. Publications Office.

71 Filiatrault A, Bachman RE and Mahoney MG (2006). "Performance-Based Seismic Design of Pallet-Type Steel Storage Racks". *Earthquake Spectra*, **22**: 47–64. https://doi.org/10.1193/1.2150233

72 Singh MP, Rildova and Suarez LE (2004). "Non-linear seismic response of the rail-counterweight system in elevators in buildings". *Earthquake Engineering Structural Dynamics*, **33**: 249–270. https://doi.org/10.1002/eqe.347

73 Wang X, Hutchinson TC, Astroza R, Conte JP, Restrepo JI, Hoehler MS and Ribeiro W (2017). "Shake table testing of an elevator system in a full-scale five-story building". *Earthquake Engineering Structural Dynamics*, **46**: 391–407. https://doi.org/10.1002/eqe.2793

74 Wang X, Günay S and Lu W (2021). "Mechanical model and seismic study of the roller guide–rail assembly in the counterweight system of elevators". *Earthquake Engineering Structural Dynamics*, **50**: 518–537. https://doi.org/10.1002/eqe.3344

75 Ayres JM and Sun TY (1973). "Nonstructural Damage, The San Fernando California Earthquake of February, 9, 1971".

76 Dames and Moore (1994). "A Special Report on the January 17, 1994 Northridge Earthquake".

77 Fathali S and Filiatrault A (2007). "Experimental Seismic Performance Evaluation of Isolation/Restraint Systems for Mechanical Equipment Part I: Heavy Equipment Study".

78 Calvi GM and Nascimbene R (2023). *Seismic Design and Analysis of Tanks*. John Wiley Sons.

79 Rashid M, Dhakal R and Sullivan TJ (2023). "Monotonic testing of brace assemblies for piping systems and considerations for capacity design". *Bulletin of the New Zealand Society for Earthquake Engineering*, **Under review**.

80 Filiatrault A, Christopoulos C and Stearns C (2001). "Guidelines, Specifications, and Seismic Performance Characterization of Nonstructural Building Components and Equipment".

81 DSA (1994). "Northridge Earthquake – Public School Buildings. Final Report".

82 Coughlin AM, Braman KM and Bergman B (2022). "Seismic Fragility Testing of Electrical Equipment for the Safe Operation of Hydroelectric Facilities". *Fifth International Workshop on the Seismic Performance of Non-Structural Elements (SPONSE)*, Stanford, California, USA.

83 Calvi PM and Ruggiero D (2017). "Earthquake-induced floor accelerations in base isolated structures". *16th World Conference on Earthquake Engineering*, Santiago, Chile.

84 Priestley M, Calvi GM and Kowalsky M (2007). *Direct displacement-based seismic design*. IUSS Press, Pavia, Italy.